frontiers | Frontiers in Earth Science

TYPE Original Research
PUBLISHED 11 May 2023
DOI 10.3389/feart.2023.1173846

OPEN ACCESS

EDITED BY
Omid Haeri-Ardakani,
Department of Natural Resources, Canada

REVIEWED BY
Karem Azmy,
Memorial University of Newfoundland, Canada
Borhan Bagherpour,
Shiraz University, Iran

*CORRESPONDENCE
Chao Chang,
changchao@nwu.edu.cn
Yanlong Chen,
yanlong.chen@nwu.edu.cn

RECEIVED 25 February 2023
ACCEPTED 25 April 2023
PUBLISHED 11 May 2023

CITATION
Yang X, Chang C, Chen Y, Topper T, Liu F, Liang Y, Fang R and Zhang Z (2023), Geochemical records and environmental analysis of the Ediacaran-Cambrian boundary in Eastern Yunnan, South China.
Front. Earth Sci. 11:1173846.
doi: 10.3389/feart.2023.1173846

Geochemical records and environmental analysis of the Ediacaran-Cambrian boundary in Eastern Yunnan, South China

Xuan Yang[1], Chao Chang[1]*, Yanlong Chen[1]*, Timothy Topper[1,2], Fan Liu[1], Yue Liang[1], Ruisen Fang[1] and Zhifei Zhang[1]

[1]State Key Laboratory of Continental Dynamics, Shaanxi Key Laboratory of Early Life and Environments, Department of Geology, Northwest University, Xi'an, China, [2]Department of Palaeobiology, Swedish Museum of Natural History, Stockholm, Sweden

The Ediacaran–Cambrian transition is characterized by an unprecedented change in biosphere, lithosphere, and atmosphere. However, the identification of this transition and its global correlation remains debated. East Yunnan is a region of utmost importance in the study of the Ediacaran-Cambrian transition. Although strata from this region have been well studied, recognition of the base of the Cambrian continues to be controversial. This paper presents, a carbon chemostratigraphic isotope and trace element profile through the Dengying and Zhujiaqing formations in the Sujiawa section in East Yunnan. Through carbon isotope and trace element analyses of the Dengying and Zhujiaqing formations we attempt to regionally correlate the section and discuss the paleo-marine redox environment changes during this period. The Fe content of samples is low and the Mn/Sr ratios of the majority of the Sujiawa section samples is lower than 10 and shows no correlations with $\delta^{13}C_{carb}$ and $\delta^{18}O_{carb}$ values, indicating that the samples retain near-primary $\delta^{13}C_{carb}$ characteristics. The carbon isotope profile from the Sujiawa section, shows a prominent negative $\delta^{13}C_{carb}$ in the basal Zhongyicun Member (N1', −7.3‰) that most likely represents the prominent negative excursion recorded in Ediacaran-Cambrian strata across the world. REE patterns and Y/Ho ratios were used to screen samples, to ensure that the primary seawater REE features and Ce anomalies were preserved. The samples satisfying this screening process show seawater-like REE distribution patterns in leached carbonates and may have recorded Ce anomalies of the seawater from which the carbonates precipitated. These data show that the Baiyanshao Member has Ce/Ce* values between 0.57 and 0.88, the Daibu Member between 0.56 and 0.83, and the Zhongyicun Member between 0.60 and 0.96. The Ce anomalies through the section indicates that the region experienced suboxic-oxic-anoxic conditions throughout the Ediacaran-Cambrian period. Carbon isotope and trace element analyses indicate that the strata record a negative carbon isotope excursion event and anoxic conditions during the period of deposition. This study complements the carbon chemostratigraphic information and trace element data in the region and provides valuable clues for understanding the lithofacies changes through the Ediacaran and Cambrian in different regions of South China.

KEYWORDS

Ediacaran, Cambrian, Dengying formation, Zhujiaqing formation, carbon isotope chemostratigraphy, trace elements chemostratigraphy, small shelly fossils, paleoenviroment

1 Introduction

The Ediacaran-Cambrian transition represents one of the most significant periods in Earth's history, which witnessed the emergence of the majority of metazoan phyla (e.g., Arthropoda, Brachiopoda, and Mollusca) present in the oceans today. This radiation in biodiversity was accompanied by a dramatic increase in ecological interactions, niche exploitation and predatory lifestyles that gave rise to the first complex metazoan-dominated marine ecosystems (Muscente et al., 2019; Wood et al., 2019; Shahkarami et al., 2020; Vaziri et al., 2021). Efforts to understand the temporal context of these significant events continue to be hindered by the inability to satisfactorily correlate key stratigraphic sections across this transition. The Global Boundary Stratotype Section and Point (GSSP) of the Ediacaran-Cambrian (E-C) boundary is currently located in the Fortune Head section in Newfoundland and defined by the first appearance of the ichnotaxon *Treptichnus pedum* (Brasier et al., 1994; Landing, 1994). Despite ratification over 30 years ago, the debate on the Ediacaran-Cambrian boundary remains a topic of heated discussion (Rozanov, 1967; Zhu, 1997; Zhu, 2001; Zhu et al., 2003; Qian et al., 2002; Peng and Babcock, 2011; Babcock et al., 2014; Topper et al., 2022). The reliability of *T. pedum* as a correlative marker has been repeatedly questioned. One of the most significant complications when employing *T. pedum* for global correlation is that of facies dependence, as *T. pedum* is predominantly confined to siliciclastic rocks (Gehling et al., 2001; Geyer, 2005; Babcock et al., 2014; Buatois, 2018; Zhu et al., 2019; Topper et al., 2022). This lithofacies dependence reduces the utility of *T. pedum* as a proxy of the base of the Cambrian, as many key regions that straddle the Ediacaran-Cambrian boundary are preserved in predominantly carbonate facies, such as China, Kazakhstan, Siberia and Mongolia (Topper et al., 2022; Bowyer et al., 2023). This has resulting in scientists frequently adopting different proxies to determine the Ediacaran-Cambrian boundary (Budd et al., 2003; Zhu et al., 2017; Darroch et al., 2018; Tarhan et al., 2018; Zhu et al., 2019; Topper et al., 2022). The use of different proxies to define the boundary has muddied the waters, highlighted the difficulty of accurately recognizing and correlating the base of the Cambrian (Landing et al., 2013; Zhu et al., 2019; Bowyer et al., 2022; Bowyer et al., 2023; Topper et al., 2022).

Ediacaran-Cambrian strata are widely distributed across the eastern Yunnan area and consequently the region has been heavily studied over the last 50 years (Ishikawa et al., 2008; Jiang et al., 2012; Li et al., 2013; Geyer, 2019; Zhu et al., 2019; Zhu et al., 2021). Nevertheless, recognition of the Ediacaran-Cambrian boundary remains difficult. Early studies placed the base of the Cambrian above the Daibu Member of the Zhujiaqing Formation, primarily due to the lack of recognizable fossils in the Daibu Member (Figure 3; Li et al., 2001; Li et al., 2009; Li et al., 2013; Zhu, 2001). The subsequent discovery of fossils, such as *Anabarites trisulcatus* generally considered as a taxon characteristic of the Cambrian, saw the base of the Cambrian pushed down into the Daibu Member (Luo et al., 1982; Zhou et al., 1997; Shen and Schidlowski, 2000; Steiner et al., 2007; Yang et al., 2016). However, the discovery of *Anabarites* and *Cloudina* co-occuring in strata in Southern Shaanxi province of South China placed uncertainty over the value of *Anabarites* as a diagnostic Cambrian taxon (Cai et al., 2019).

With uncertainty surrounding the first appearance of key Cambrian fossils, carbon isotope chemostratigraphy has been increasingly utilized to recognize the base of the Cambrian and promote regional and international correlation (Shen and Schidlowski, 2000; Li et al., 2009; Li et al., 2013). A pronounced negative carbon isotope excursion has been repeatedly recorded across numerous stratigraphic sections in Yunnan, such as the Laolin and Xiaotan sections (Li et al., 2009; 2013). This prominent excursion in the Ediacaran and Cambrian strata of Yunnan has been referred to as the L1' (Li et al., 2009) or the N1 (Li et al., 2013) excursion and has been correlated with an excursion that has been documented from many sections around the world, referred to widely as the BACE (Basal Cambrian carbon isotope Excursion; see Zhu et al., 2006; Zhu et al., 2019). Often used as a proxy to identify the base of the Cambrian, the presence of this excursion, would place the Ediacaran-Cambrian boundary in the basal Daibu Member of the Zhujiaqing Formation (Li et al., 2009; Li et al., 2013; Zhu et al., 2019). However, to complicate issues, the siliceous dolostone at the base of the Zhujiaqing Formation in some localities unconformably overlies the massive dolostone at the top of the Dengying Formation, frequently obscuring the proposed boundary (Zhu et al., 2021) and as such, the Ediacaran-Cambrian boundary in South China is still uncertain.

Although the precise temporal relationship between fossil taxa from the Ediacaran and the Cambrian remains unresolved, it is widely believed that changes in the global ocean environment were important factors influencing the early evolution of animals (Grotzinger et al., 1995; Knoll and Carroll, 1999; Amthor et al., 2003; Marshall, 2006; Maloof et al., 2010; Wang et al., 2012). Together with the pronounced negative carbon isotope excursion, previous studies have identified negative Ce anomalies in carbonates (Komiya et al., 2008) and the enrichment of redox sensitive V and U in shelf sediments (Kimura and Watanabe, 2001) providing evidence for fluctuating conditions in the marine environment. In particular, negative Ce anomalies and the enrichment of redox sensitive V and U indicate periods of anoxia in the shallow seas during the Ediacaran-Cambrian (Kimura and Watanabe, 2001; Komiya et al., 2008). However, a variety of other factors have been suggested to explain these chemical anomalies such as, increased particulate organic carbon produced by plankton (Rothman et al., 2003), catastrophic methane release (Bartley et al., 1998), upwelling of euxinic bottom waters (Wille et al., 2008; Chang et al., 2017), and sealevel transgressions (Zhu et al., 2004).

Here, in order to improve our understanding of the paleoenvironmental conditions on the Yangtze Platform and to promote stratigraphic correlation across the platform we present a $\delta^{13}C$ chemostratigraphic profile through the Denying and Zhujiaqing formations at the Suijawa section in South China. This study additionally integrates trace element data to provide a new perspective on the Ediacaran-Cambrian boundary in eastern Yunnan. The paleoredox conditions of strata through the section were assessed using the ratio of key trace elements. The significance of these results in regards to the palaeoenvironmental interpretation of the Suijawa section is discussed.

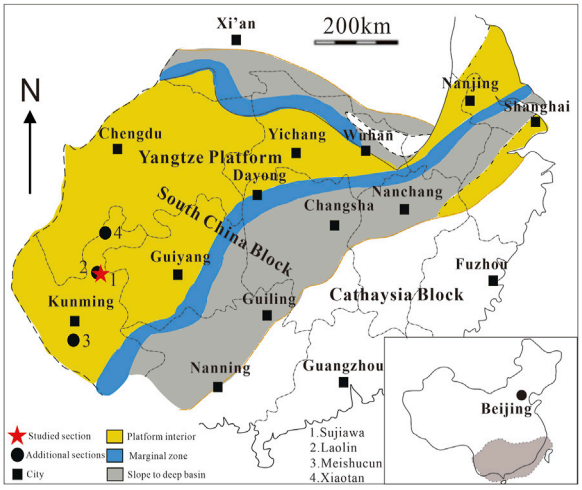

FIGURE 1
Simplified geological map of the Sujiawa section, Huize county, Yunnan province, South China. Paleogeographical map of Huize area. Showing the location of 1) the Sujiawa section; 2) the Laolin section; 3) the Meishucun section; 4) the Xiaotan section (modified from Zhu et al., 2003; Li et al., 2013).

2 Geological setting, stratigraphy

The study area is located in the southwest of the Yangtze Platform with a paleogeographic position of about 11–18°S (Figures 1, 2; Chen et al., 2002). The late Ediacaran to early Cambrian strata in this area have been interpreted as recording predominantly a continuous transgressive sedimentary sequence (Qian et al., 1996; Zhu et al., 2003; Zhu et al., 2007; Zhou et al., 2017; Yang and Steiner, 2021). The South China Plate deepens from the northwest to the southeast, and can be divided into three parts: the platform interior, marginal zone and slope to the deep basin (Zhu et al., 2003). Strata in eastern Yunnan have experience extensive tectonic activity and many of the previously studied sections (e.g., Laolin, Xiaotan and Meishucun sections) are separated by significant faults (Tian, 1990), that has impeded correlation. The lithology of Ediacaran-Cambrian strata also varies across the platform, however a generalized sequence consists of the Dengying Formation, the overlying Zhujiaqing Formation (including the Daibu, Zhongyicun and Dahai members), followed by the Shiyantou and Yuanshan formations (Figure 3). The Dengying Formation, that includes the Donglongtan, Jiucheng and Baiyanshao members is mainly comprised of dolostone. The Donglongtan Member is predominantly dolostone, and is overlain by the shales of the Jiucheng Member. The Baiyanshao Member comprises thickly bedded to massive dolostone (Qian et al., 1996). Contact with the overlying Zhujiaqing Formation is frequently unconformable, but where preserved the base of the overlying Zhujiaqing Formation is defined by the presence of siliceous dolostone (Qian et al., 1996; Zhu, 2001). The Zhujiaqing Formation contains three members; the Daibu, Zhongyicun and Dahai members. The Daibu Member comprises siliceous dolostone with some interbedded dolomitic chert horizons. The Zhongyicun Member is predominantly grey, thick beds of phosphorites and the base of the member is defined by the first presence of phosphorite (Qian et al., 1996). The Dahai Member predominantly comprises thickly bedded limestone. The overlying Shiyantou Formation, not sampled in the Sujiawa section, comprises thickly to thinly bedded quartz siltstone (Zhu, 2001).

The Sujiawa section (GPS: N26°22′40.7″, E: 103°12′48.2″) is located near Dahai, Huize County, northeast of Kunming city, Yunnan Province (Figures 1, 2). The Sujiawa section commences at the base of the Baiyanshao Member and continues through the Daibu and Zhongyicun members with a total true thickness of 161 m (Figure 4). The Baiyanshao Member is 64.3 m in true thickness, and can be divided into two parts; the lower part is composed of medium-thin layer dolostones and the upper part consists of medium-thin-layer limestone beds. Limestone beds have not been previously documented from the upper Baiyanshao Member in East Yunnan and are a unique lithology to this locality (Figure 4). The Zhujiaqing Formation conformably overlays the Baiyanshao Member of the Dengying Formation. In the Zhujiaqing Formation, the Daibu Member is composed of medium-thin-layer siliceous dolostones with black cherts and the member is approximately 23.1 m in true thickness. The Zhongyicun Member is composed of phosphorites with a thickness of 70 m (Figure 4).

3 Materials and methods

All samples in this study were collected from the Sujiawa section in Huize County, Yunnan Province. A total of 65 rock samples were collected from the Baiyanshao Member to the Zhongyicun Member, of which 37 were from the Baiyanshao Member, 14 were from the Daibu Member, and 14 were from the Zhongyicun Member (Figure 4).

At each sampled horizon, material was collected for shelly fossil, isotope and trace element analysis. Of the total 65 samples, 19 samples were excluded from the carbon isotope analysis because they lacked sufficient carbonate minerals. Three samples were lost and hence also omitted from the elemental (include trace element) analysis. Thin sections of rock samples were inspected under a polarizing microscope in order to identify visible alterations such as calcite micro-veins and areas of recrystallized calcite, so these regions can be avoided when performing elemental and isotopic analyses. Samples were then cut to get access to a fresh surface that were microdrilled to obtain powder for analysis, with 10–20 g extracted from most samples. Quartz and feldspar veins were deliberately avoided, ensuring that the best possible primary signal would be obtained. The prepared samples were then placed into a sample bag for carbon and oxygen isotope and major and trace element analyses.

3.1 Carbon isotope analysis

Sample testing was performed using a Thermo Scientific 253 Plus isotope ratio mass spectrometry (IRMS) system equipped with Gas Bench II (Gas Bench-IRMS) at the State Key Laboratory of Continental Dynamics at Northwestern University.

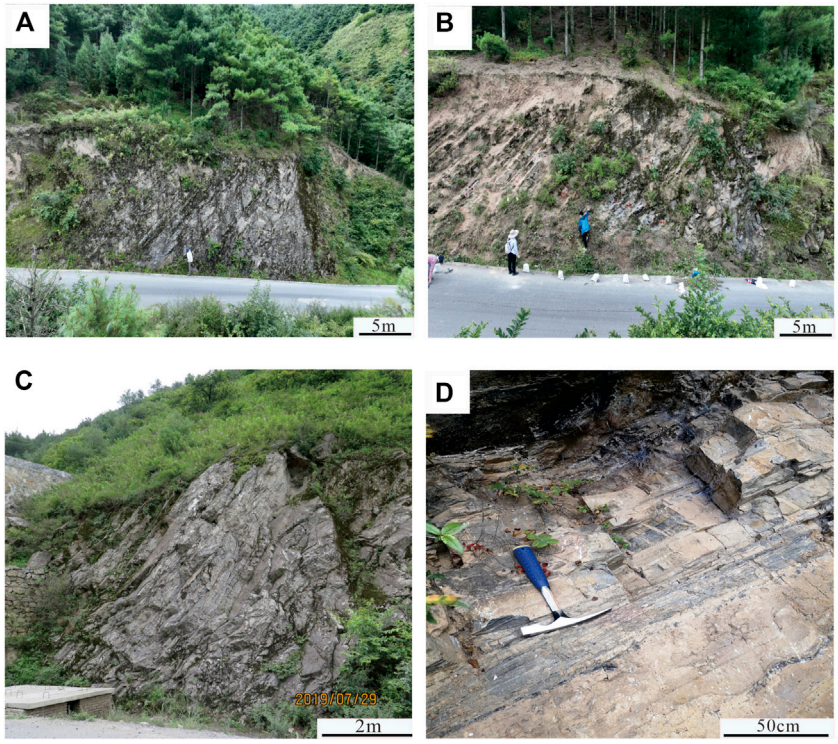

FIGURE 2
Outcrop pictures of the Sujiawa section, Huize county, Yunnan province, South China. **(A)** Outcrop of medium - thin white and grey dolomite in the lower part of Baiyanshao Member; **(B)** Outcrop of medium-thin limestone intercalated with calcareous shale in the upper part of Baiyanshao Member; **(C)** Outcrop of siliceous dolostone in the Daibu Member; **(D)** Outcrop of phosphorite in the Zhongyicun Member.

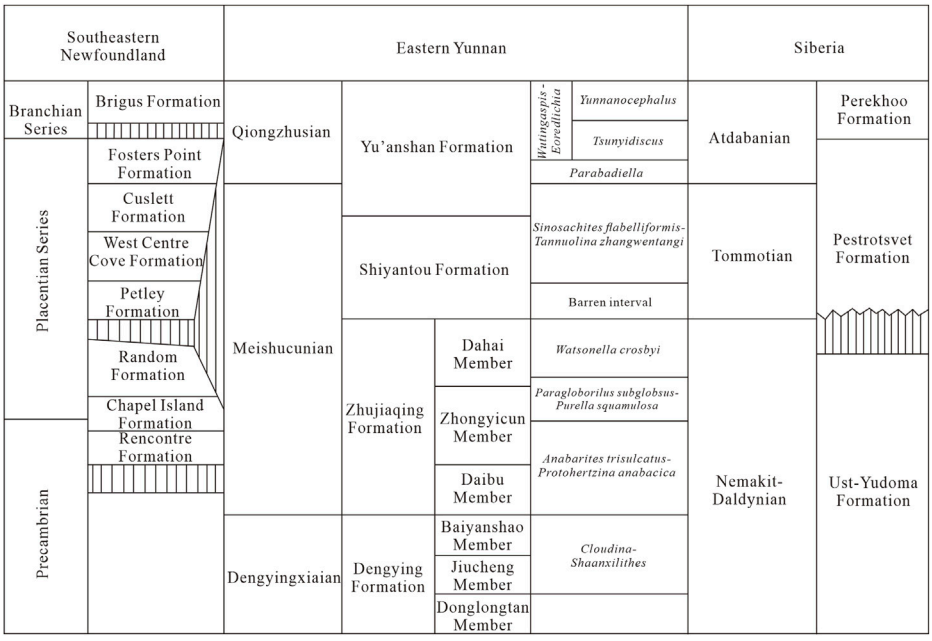

FIGURE 3
Stratigraphic correlation of strata during the Precambrian to early Cambrian across South China, Siberia and southeastern Newfoundland (modified from Zhu, 2001; 2019; 2021). The Sujiawa section is located in eastern Yunnan, and the stratigraphic successions, in ascending order, consist of the Dengying Fm. (Baiyanshao Mb.), Zhujiaqing Fm. (Daibu Mb., Zhongyicun Mb., Dahai Mb.).

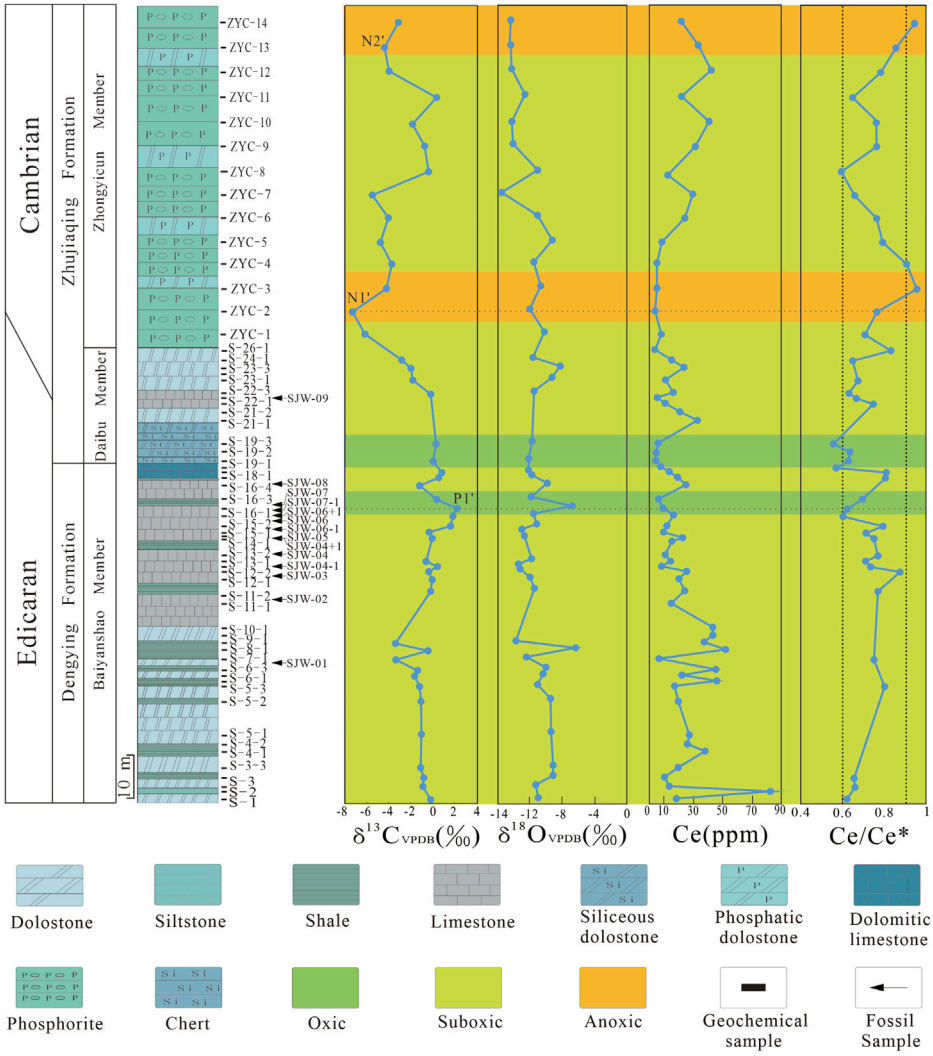

FIGURE 4
Stratigraphic column, carbon isotope and trace element characteristics of Ediacaran-Cambrian strata in the Sujiawa section, Huize county, Yunnan province, South China.

All samples consist of 100 μg of powder that was placed into a glass vial and reacted with phosphoric acid for 2 h at 70°C. Generated CO_2 gas was transferred to IRMS for measurement with helium for carrier gas. The IRMS is able to run 16 samples consecutively and 2 standards were inserted every 6 samples for isotopic calibration. Each standard sample was analyzed ten times. The analytical results were calibrated by Chinese reference standard GBW04405 ($\delta^{13}C_{carb}$= 0.57‰, $\delta^{18}O_{carb}$= −8.49‰). The analytical standard deviation of values from 10 repeated analyses were under 0.2‰ and 0.3‰, respectively. Isotopic data are reported in delta notation relative to the international Vienna Pee Dee Belemnite (VPDB) standard for $\delta^{13}C_{carb}$ and $\delta^{18}O_{carb}$.

3.2 Major and trace element analysis

Major and trace element analyses were undertaken at the State Key Laboratory of Continental Dynamics at Northwest University following the protocol of Wang and Liu (2016). A small part of each sample was added to the flux including lithium borate, lithium fluoride and ammonium nitrate, mixed thoroughly and poured into the platinum tray. Lithium bromide (0.15 mg) was then added and melted on the fusion machine at high temperatures. After the melt had cooled to form a flat glass sheet, RIX2100X fluorescence spectrometer (XRF) was used to analyze the content of major elements. The relative deviation of the analyses was under 5‰.

The whole rock trace element analysis was also completed at the State Key Laboratory of Continental Dynamics at Northwest University. The samples were initially ground through a 200 mesh. Sample powders (50 mg) were weighed in 25 mL tubes for dissolution using 3 mol/L acetic acid and shaken at room temperature. The reaction time was approximately 12 h, which was sufficient to ensure a complete reaction. The insoluble residues were separated by centrifugation and ultrapure water

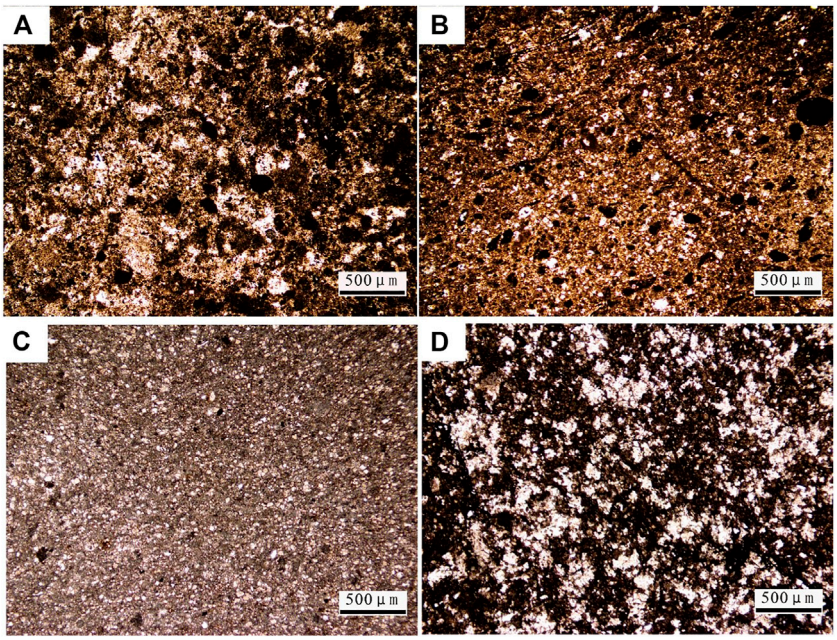

FIGURE 5
Microscopic photos of the rocks in the Sujiawa section, Huize county, Yunnan province, South China. **(A, B)** Phosphatic dolostone in the Zhongyicun Member (ZYC-1 and ZYC-3); **(C)** Limestone in the upper part of Baiyanshao Member (S-11-1); **(D)** Dolostone in the middle and lower part of Baiyanshao Member (S-5-1).

was then added to the previous supernatant and dried again to remove the remaining acetic acid. ELAN6100DRC ICP-MS was used for testing and analysis, and Rh was used as an internal standard to monitor the signal drift during measurements. The relative deviation of the analyses was under 5‰.

4 Results

4.1 Petrographic preservation

Microscopic observations of samples are necessary for identifying the sample lithology and for choosing the appropriate rock component for geochemical analysis. Petrographic images of horizons through several members can be seen in Figure 5 and are described as follows. The lower Baiyanshao Member predominantly contains dolosparite, dolomicrosparite, and partially recrystallized dolomicrosparite (Figure 5D). The upper Baiyanshao Member contains sparite, microsparite, and partially recrystallized pelsparite. (Figure 5C). The overlying Zhongyicun Member is typically a phosphorite-bearing member of the Zhujiaqing Formation. Phosphate in the Zhongyicun Member can instantly be recognized in thin section (Figures 5A,B).

4.2 Carbon isotopes

The C- and O-isotope and trace element results are listed in Supplementary Table S1. The $\delta^{13}C_{carb}$ profile of the Sujiawa section is presented in Figure 4. $\delta^{13}C_{carb}$ values of the lower part of the Baiyanshao Member of the Dengying Formation remain predominantly steady but show a general decline from 0‰ to −2‰ until the middle part of the middle member where there is a small fluctuation, with a maximum value of $\delta^{13}C_{carb}$ at −0.52‰ and a minimum value is −3.44‰. The $\delta^{18}O_{carb}$ values of the lower part of the Baiyanshao Member of the Dengying Formation range from −6.52‰ to −13.91‰. In the upper part of the Baiyanshao Member, a prominent positive $\delta^{13}C_{carb}$ excursion occurs with a maximum value of 2.11‰, followed by a small negative $\delta^{13}C_{carb}$ excursion with a minimum value of −1.30‰. $\delta^{13}C_{carb}$ values rise slightly to 0.73‰ in the uppermost Baiyanshao Member. The $\delta^{18}O_{carb}$ values of the upper part of the Baiyanshao Member range from −6.94‰ to −13.35‰. In the Daibu Member, $\delta^{18}O_{carb}$ values range from −8.58‰ to −12.36‰ and $\delta^{13}C_{carb}$ values are stable in the range of 1‰ ~ −1‰, before a gradual decline in values ending in a pronounced negative $\delta^{13}C_{carb}$ excursion of −7.3‰ at the base of the overlaying Zhongyicun Member. $\delta^{13}C_{carb}$ values then rise to −3.8‰, fluctuating between −3.8‰ and −5.6‰ for the next 20 m (true thickness) of the Zhongyicun Member. In the middle part of the Zhongyicun Member, a weak positive $\delta^{13}C_{carb}$ excursion occurs, with the maximum value of 0.2‰. The $\delta^{13}C_{carb}$ record fluctuates between −1.9‰ and 0.2‰ for the remainder of the Zhongyicun Member before another negative $\delta^{13}C_{carb}$ excursion at the top of Zhongyicun Member, with a minimum value of −4.5‰ (Figure 4). The $\delta^{18}O_{carb}$ values of the Zhongyicun Member ranges from −9.26‰ to −14.44‰.

4.3 Major and trace element analysis

The Mn and Fe values are listed in Supplementary Table S1; Figure 6. The Mn values in the Baiyanshao Member are 0.77–5.42 ppm. The Mn

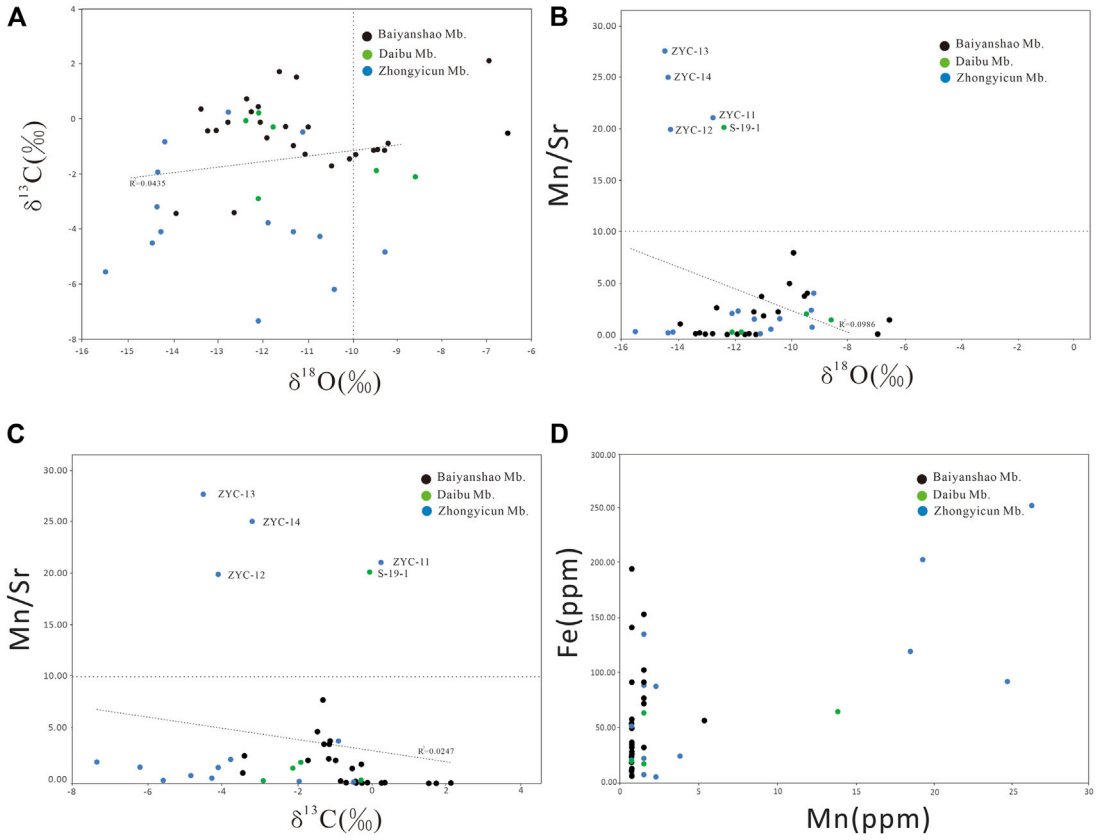

FIGURE 6
Correlation analysis of $\delta^{13}C$, $\delta^{18}O$ and Mn/Sr of Baiyanshao Member, Daibu Member and Zhongyicun Member in the Sujiawa section, Huize county, Yunnan province, South China. **(A)** Cross plot of $\delta^{13}C$-$\delta^{18}O$; **(B)** Cross plot of Mn/Sr-$\delta^{18}O$; **(C)** Cross plot of Mn/Sr-$\delta^{13}C$; **(D)** Cross plot of Fe-Mn.

values in the Daibu Member are 0.77–13.94 ppm. The Mn values in the Zhongyicun Member are 0.77–26.34 ppm. The Fe values in the Baiyanshao Member are 7.00–194.60 ppm. The Fe values in the Daibu Member are 17.50–65.10 ppm. The Fe values in the Zhongyicun Member are 5.60–252.00ppm.

Figure 4 shows the cerium anomaly analysis through the Sujiawa section. The REEs are normalized to Post-Archean Australian Shale (PAAS) (Taylor and McLennan, 1985). In our analysis, the formula for the cerium anomaly is: $Ce/Ce^{*} = Ce_n/\mathrm{Pr}_n\,\mathrm{Pr}_n^{\hat{}2}/Nd_n$ (Lawrence et al., 2006) and Ce/Ce* values varied between 0.558 and 0.971 (Supplementary Table S2).

The trend of Ce (ppm) through the Sujiawa section is shown in Figure 4. Some Ce anomalies are shown in Figure 4 with data showing high Y/Ho ratios (>36), samples with ratios elevated above the detrital background, showing a strong seawater REE signal (Tostevin et al., 2016; Cherry et al., 2022). Regarding paleo-oceans, Ce anomalies up to 0.3-0.6 are considered to be oxic environments, and values >0.9 are considered to represent anoxic environments, and ratios between 0.6 and 0.9 are considered to indicate suboxic environments (Ling et al., 2013). The Ce/Ce* values of the Dengying Formation in the Sujiawa section (Figure 4) are 0.57–0.88. The Ce/Ce* values of the lower and middle samples of the Baiyanshao Member of the Dengying Formation are 0.62–0.83. The Ce/Ce* values of the upper part of the Baiyanshao Member of the Dengying Formation are 0.57–0.88. The Ce/Ce* values of the Daibu Member are 0.56–0.83, and the Ce/Ce* values through the majority of the Zhongyicun Member are 0.60–0.96. The top of the Zhongyicun Member displays high values that are above 0.9 (Figure 4).

5 Discussion

5.1 Diagenetic evaluation

Before using carbon isotopes for reliable stratigraphic correlation and palaeoenvironmental reconstruction, it is important to assess for diagenetic alteration to ensure that the isotopic characteristics of primary carbonate are preserved (Derry et al., 1994; Kaufman and Knoll, 1995; Bartley et al., 1998; Veizer et al., 1999; Wotte et al., 2007). Thin sections of samples through the Sujiawa section (Figure 5) do not show high levels of recrystallisation that indicates that the carbonates, have undergone limited diagenetic modifications. Meteoric diagenesis can lead to Mn and Fe enrichment and Sr depletion in marine carbonate rocks (Brand and Veizer, 1980; Veizer, 1983; Azmy et al., 2011). Thus, the Mn/Sr ratio and the Mn, Fe content are frequently employed to distinguish diagenetically altered samples from unaltered samples. It is generally accepted that samples that display a Mn/Sr ratio of less than 10, indicate that they have not

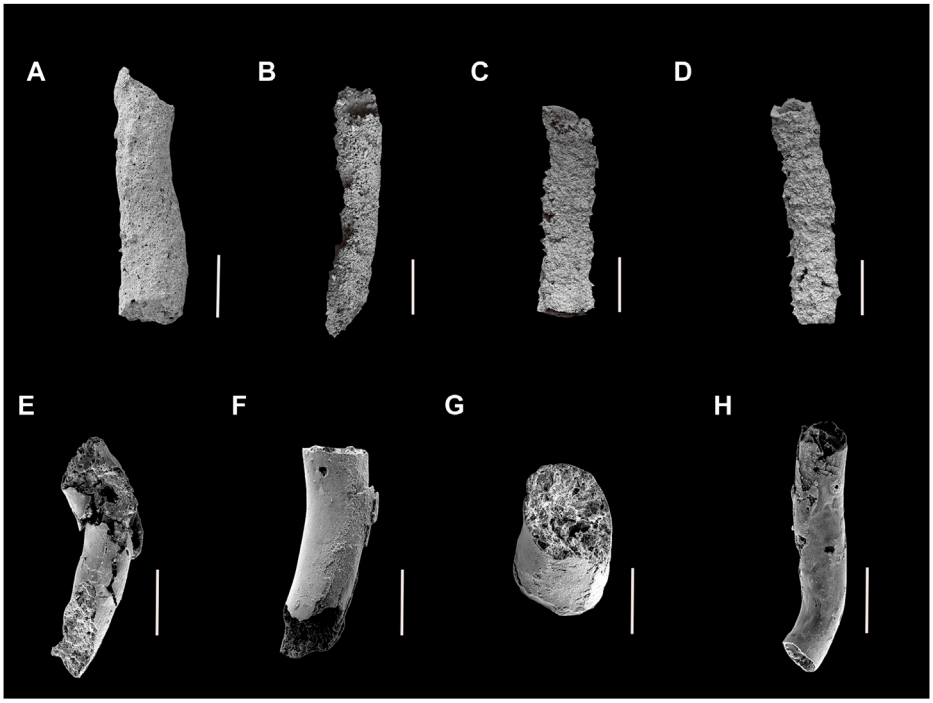

FIGURE 7
SEM images of tubular fossils derived from the Baiyanshao Member **(A–D)** to the Daibu Member **(E–H)** in the Sujiawa section, Huize county, Yunnan province, South China. **(A–D)** from SJW-01, SJW-02, SJW-06, SJW-06+1; **(E–H)** from SJW-09. Scale bars: 500 μm **(A,E,F,G and H)**, 1 mm **(B–D)** All fossils are deposited at the Department of Geology, Northwest University, Xi'an, China.

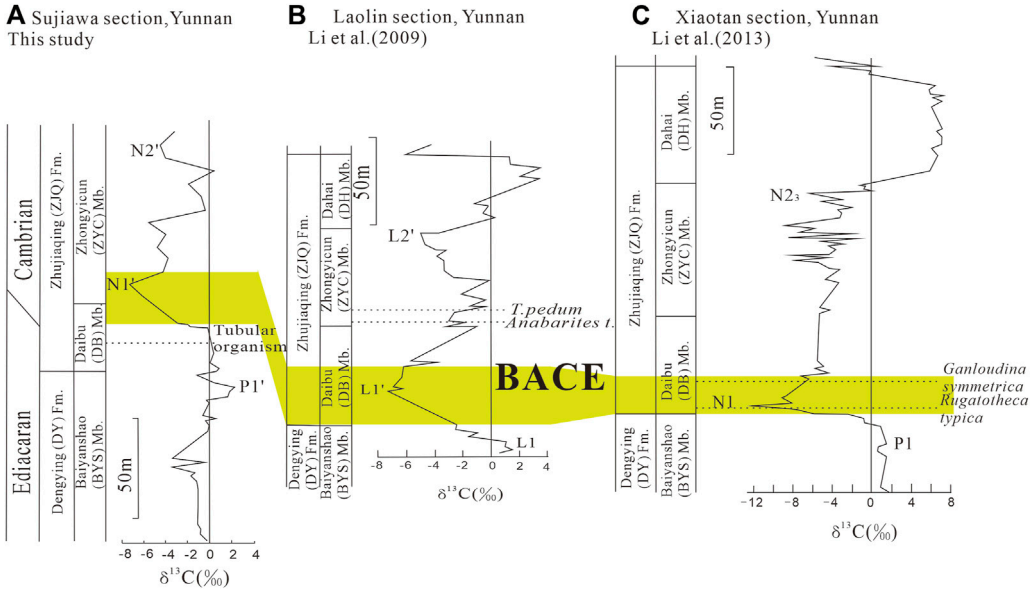

FIGURE 8
C-isotope stratigraphic correlation scheme between sections on the Yangtze platform. **(A)** Yunnan Sujiawa section, this study; **(B)** Yunnan Laolin section, Li et al., 2009; **(C)** Yunnan Xiaotan section (carbon isotopes combine with SSF zone), Li et al., 2013; Yang et al., 2016.

undergone late diagenesis (Kaufman and Knoll, 1995; Bartley et al., 1998; Azmy et al., 2014). In addition to Mn/Sr ratios, progressive diagenesis can also lead to $^{13}C_{carb}$ and $\delta^{18}O_{carb}$ depletion in marine carbonates, so the $\delta^{18}O_{carb}$ value and its correlation with the $\delta^{13}C_{carb}$ value can be used to evaluate the preservation of the original carbon isotopic signature (Bathurst,

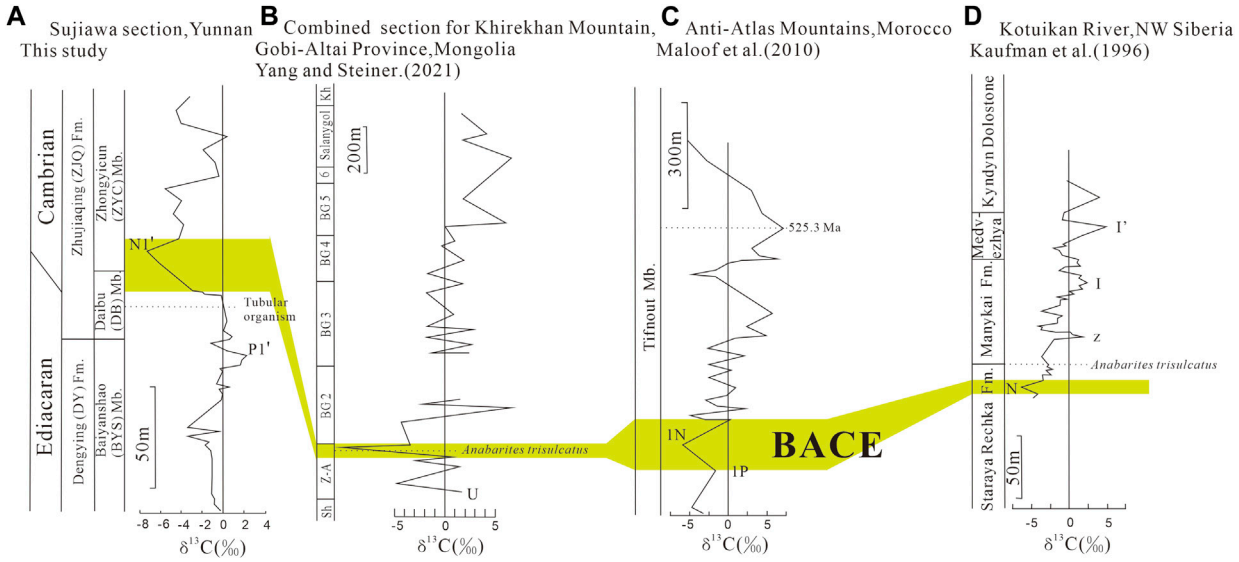

FIGURE 9
Global carbon stratigraphic correlation scheme in the early Cambrian. **(A)** Yunnan Sujiawa section, this study; **(B)** Khirekhan Mountain in Mongolia, Yang et al., 2020; Brasier et al., 1994; **(C)** Anti-Atlas Mountains in Morocco, Maloof et al., 2010; **(D)** Kotuikan River in NW Siberia, Kaufman and Knoll, 1995.

1975; Kaufman and Knoll, 1995; Li et al., 2009). Carbonates that have not undergone a significant diagenetic transformation (Veizer et al., 1999) typically show $\delta^{18}O^{carb}$ values of > −10‰. In addition, if $\delta^{13}C_{carb}$ and $\delta^{18}O_{carb}$ values do not show a positive correlation, it is also a good indicator that the carbonate rocks have retained their original chemical composition (Kaufman and Knoll, 1995).

As shown in Figure 6, almost half of our carbonate $\delta^{18}O_{carb}$ values are < −10‰. In early isotopic studies, these low values would have been considered to represent diagenesis alteration (Derry et al., 1992; Derry et al., 1994; Kaufman and Knoll, 1995), however in recent studies these values have been reevaluated. The $\delta^{18}O_{carb}$ values of a large number of Cambrian carbonates are also reported to be less than 10‰, but their corresponding $\delta^{13}C_{carb}$ values are still considered to reflect the near-primary carbon isotope signal (Dillard et al., 2007; Wotte et al., 2007; Guo et al., 2010; Li et al., 2013; Ishikawa et al., 2014; Chang et al., 2017). It has been suggested, that this may be related to the different sensitivity of oxygen and carbon isotopic compositions of carbonate rocks to diagenesis (Kaufman and Knoll, 1995; Chang et al., 2017). Carbonate oxygen isotopes are more sensitive to diagenesis and isotopic exchange between carbonate and diagenetic fluids or hydrothermal fluids, which can result in significant negative excursions of carbonate $\delta^{18}O_{carb}$ values (Kaufman and Knoll, 1995; Veizer et al., 1999). In contrast, carbonate carbon isotopes are more robust to diagenetic alteration and more likely to preserve the near-primary signature (Derry et al., 1994; Kaufman and Knoll, 1995; Wotte et al., 2007; Ishikawa et al., 2014). Thus, although the $\delta^{18}O_{carb}$ signature can be used to trace diagenetic alteration, a threshold of values lower than −10‰ may not be suitable for distinguishing altered carbonates, at least for Cambrian strata (Chang et al., 2017). Consequently, the relationship between carbon and oxygen isotopes is seen as a more significant indicator of diagenesis for early Paleozoic carbonates. A cross-plot of $\delta^{13}C_{carb}$ and $\delta^{18}O_{carb}$ values, shows no positive correlation (r^2=0.04), suggesting that there was restricted influence of diagenetic alteration on $\delta^{13}C$ values in the Sujiawa section (Dillard et al., 2007; Guo et al., 2010; Li et al., 2013).

The Mn/Sr ratio of the majority of Sujiawa section samples is lower than 10 (based on 10 analyses per sample) and shows no correlations with $\delta^{13}C_{carb}$ (r^2=0.02) and $\delta^{18}O_{carb}$ (r2=0.09) values, indicating that the samples retain near-primary $\delta^{13}C_{carb}$ characteristics (Figure 6; Supplementary Table S1; Derry et al., 1992; Kaufman and Knoll, 1995; Bartley et al., 1998; Azmy et al., 2014; Chang et al., 2017). This data however, excludes the measurement errors caused by lithological factors (insignificant carbonate available). Although some samples are siliceous carbonates and phosphorous carbonates, only one Daibu Member and four Zhongyicun Member samples had Mn/Sr ratios higher than 10 (Figure 6). One sample however (Daibu Member 19-1), did display severe diagenesis (high Mn/Sr ratio) and subsequently this point was removed. However, samples from the Zhongyicun Member are obtained from phosphorites and consequently the measurements of their major elements will most likely be greatly disturbed, so the accuracy of the Mn/Sr ratios of these 4 samples of Zhongyicun Member is questioned. As can be seen from Figure 6, there is little difference between the carbon and oxygen isotopes of the 4 samples from the Zhongyicun Member compared with the previous samples, suggesting that diagenetic overprinting of these samples is not too severe to warrant exclusion. In addition, the low content of Mn and Fe in the samples (Supplementary Table S1; Figure 6D) reflect the limited influence of diagenesis on those carbonates.

In conclusion, it is here considered that the $\delta^{13}C_{carb}$ values presented here have undergone limited diagenesis and preserve

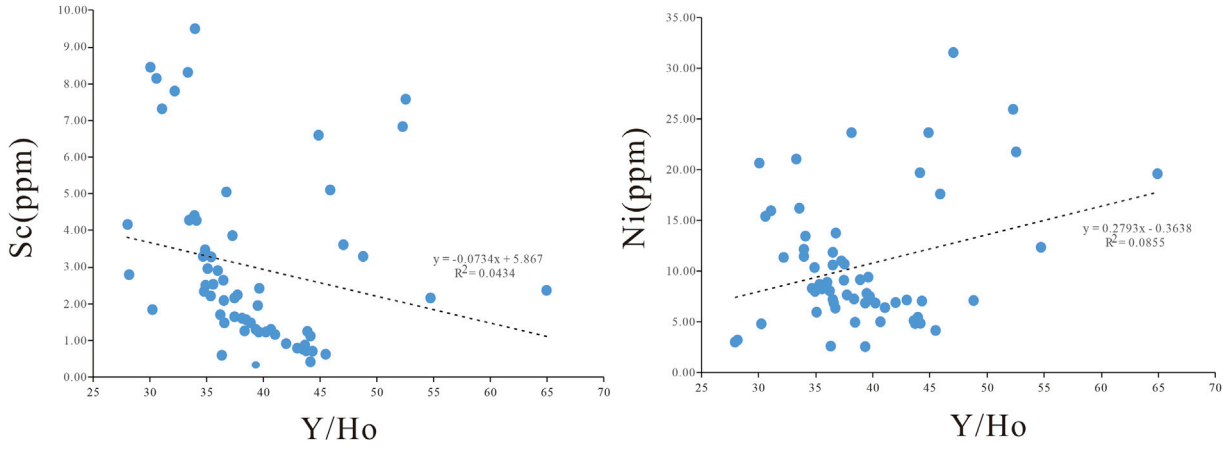

FIGURE 10
Relationship of Y/Ho ratios to concentrations of Sc and Ni in leachates form carbonate rocks from the Sujiawa section, Huize county, Yunnan province, South China.

values close to the near-primary signal, promoting use in stratigraphic correlations and paleo-environmental reconstructions.

5.2 Stratigraphic correlation

5.2.1 Regional chemostratigraphic correlation

$\delta^{13}C$ chemostratigraphic profiles of the Ediacaran-Cambrian boundary interval have been presented for numerous sections across eastern Yunnan Province, most notably from the Meischucun, Xiaotan and Laolin sections (Braiser et al., 1990; Zhu, 1997; Li et al., 2009; Li et al., 2013). The locations of these sections in relation to the Sujiawa section can be seen in Figure 1. The similarities in the $\delta^{13}C$ chemostratigraphic profiles of the Xiaotan and Laolin sections have been discussed previously with specific excursions promoting accurate correlations between the sections (Li et al., 2009; Li et al., 2013; Topper et al., 2022). Palaeontologic and $\delta^{13}C$ data from the Meishucun section (Figures 1, 3) however, suggests that there is a depositional discontinuity below the base of the Zhongyicun Member (Figures 1, 3; Li et al., 2009; Li et al., 2013; Geyer, 2019; Steiner et al., 2020; Zhu et al., 2019; Zhu et al., 2021; Bowyer et al., 2022) and the large negative excursion at the base of the Cambrian (preserved in the Laolin and Xiaotan sections) is not recorded at the Meischucun section (Li et al., 2009).

It has been shown that the strata at each section across the Yangtze platform during the Ediacaran- Cambrian transition shows some variation in lithology (Zhu et al., 2021; Figure 7). In some sections like the Meishucun section, Xiaoshiba section and Yiliang section, the Zhujiaqing Formation (generally considered to be basal Cambrian in age) unconformably overlies the Dengying Formation. However, some sections preserve a comformable contact between the Zhujiaqing Formation and the Dengying Formation, such as Laolin section and the Xiaotan section. In our section the Zhujiaqing Formation also conformably overlies the Dengying Formation and consequently the Sujiawa section can be correlates well with the Laolin and Xiaotan section, in regards to lithology. Also, the $\delta^{13}C$ chemostratigraphic profile of the Sujiawa section (Figure 4) bears a number of similarities to the Laolin and Xiaotan sections (see Figure 8) and a number of significant peaks and excursions (e.g., L1 ′, N1, N1′ and L1, P1, P1′) can be confidently recognized between the sections. All three sections (Figure 8; Li et al., 2009; Li et al., 2013) show a small positive $\delta^{13}C$ excursion in the Baiyanshao Member of Dengying Formation (L1, P1′ and P1), followed by a large negative $\delta^{13}C$ excursion (L1′, N1′ and N1). The majority of the Zhongyicun Member records negative $\delta^{13}C$ values with another marked negative $\delta^{13}C$ excursion (N_{23}, L_2', N_2') (however not as pronounced as the previous excursion) recorded in the mid to upper Zhongyicun Member (Figure 8). The Ediacaran-Cambrian boundary demarcation in eastern Yunnan has been contentious (Luo et al., 1982; Zhou et al., 1997; Shen and Schidlowski, 2000; Steiner et al., 2007). In the absence of reliable first occurrences of *T. pedum*, the base of the Cambrian in South China has frequently been associated with the first appearance of shelly fossils, in particular fossils of the *A. trisulcatus-Protohertzina anabarica* Assemblage Zone (*A. trisulcatus*, *Prohertzina anabarica*, *Prohertzina unguliformis*, *Ganloudina symmetrica*, *Rugatotheca typica*) (Figure 3; Steiner et al., 2007; Steiner et al., 2020; Yang et al., 2016; Yang and Steiner, 2021; Zhu et al., 2017). The base of the *A. trisulcatus-P. anabarica* Assemblage Zone in East Yunnan had been recorded in the Zhongyicun Member of the Zhujiaqing Formation (Figure 3; Steiner et al., 2007; 2020; Yang et al., 2016; Yang and Steiner, 2021; Zhu et al., 2017). More recently, $\delta^{13}C$ chemostratigraphy has been implemented in many studies to aid correlation across the Yangtze Platform of South China (Brasier et al., 1990; Ishikawa et al., 2008; Li et al., 2009; Li et al., 2013; Steiner et al., 2020). In particular, in East Yunnan Li et al. (2009), Figure 2; Li et al. (2013), Figure 3) placed the Ediacaran-Cambrian boundary between the Daibu Member and the Zhongyicun Member of the Zhujiaqing Formation (Figure 3) based on its association with a pronounced negative $\delta^{13}C$ excursion

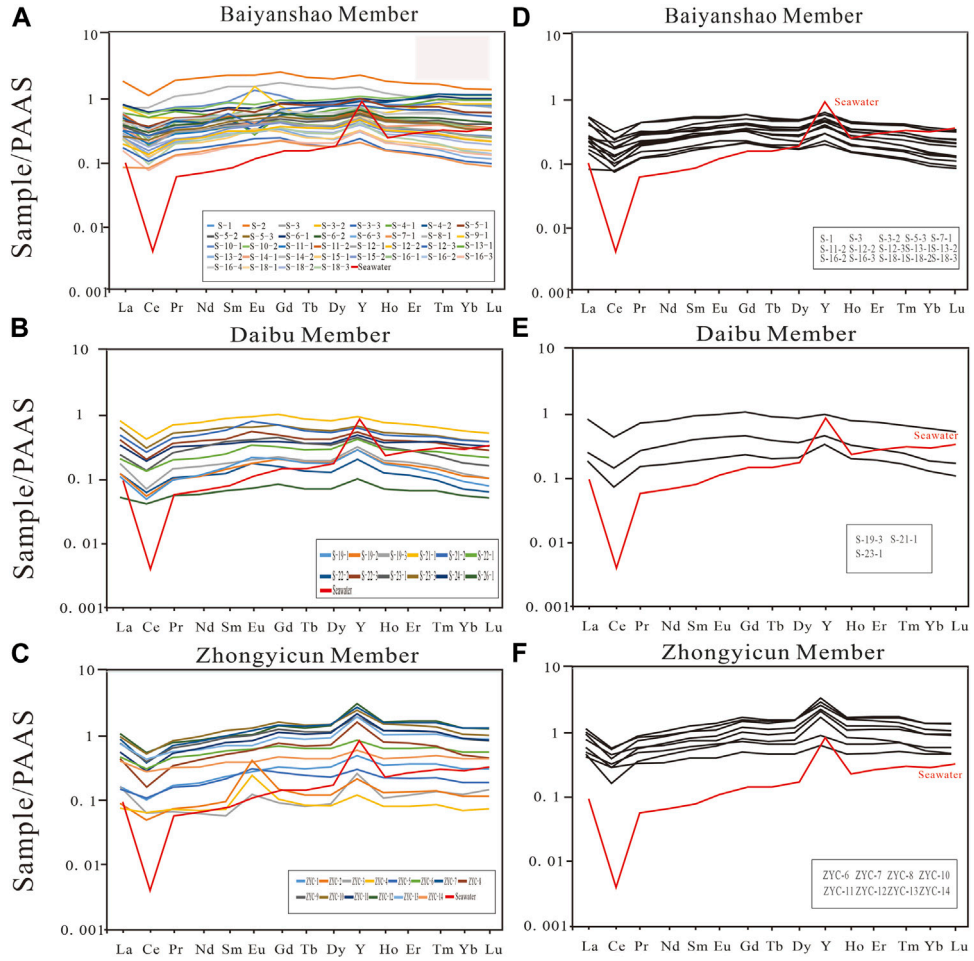

FIGURE 11
PAAS normalized REE+Y distribution patterns of the Baiyanshao Member, Daibu Member and Zhongyicun Member in the Sujiawa section, Huize county, Yunnan province, South China. **(A–C)** show the patterns for all samples; **(D–F)** shows the patterns for sample that satisfy the criteria discussed in the text. (PAAS normalized REE+Y distribution patterns of sea water was expanded 107 times).

(Figure 8, L1′ and N1) in the Daibu Member. Subsequent studies have documented shelly fossils (such as *G. symmetrica* and *Rugatotheca typical*) in the Daibu Member in the Xiaotan section (Yang et al., 2016), that were assigned to the *A. trisulcatus-P. anabarica* Assemblage Zone. This discovery saw the base of the Cambrian moved towards the contact between the Daibu Member of the Zhujiaqing Formation and the underlying Dengying Formation (Yang et al., 2016; Figure 8). However, as the contact between the two formations (Zhujiaqing Formation and Dengying Formation) is not conformable and the thickness of the Daibu Member varies considerably across the platform (Yang et al., 2016), uncertainties regarding the boundary persists. Despite these uncertainties the close association of the first appearance of shelly taxa characteristic of the *A. trisulcatus-P. anabarica* Assemblage Zone together with the presence of a pronounced negative $\delta^{13}C$ excursion (L1', N1) indicates that the Ediacaran-Cambrian boundary in the eastern Yunnan region of South China is most likely placed within the Daibu Member of the Zhujiaqing Formation (Zhuravlev et al., 2012; Yang et al., 2016; Zhu et al., 2017; Yang and Steiner, 2021; Topper et al., 2022).

Compared with the Xiaotan section (Li et al., 2013) and the Laolin section (Li et al., 2009), the overall trend of carbon isotopes in the Sujiawa section during the Ediacaran-Cambrian transition is similar. All three sections show a stable positive period from the upper part of Dengying Formation followed by a negative excursion in the Zhujiaqing Formation (Figure 8). The main difference however, is that the nadir of the negative $\delta^{13}C_{carb}$ excursion in the Sujiawa section occurs in what the authors have interpreted as the basal Zhongyicun Member, while in the Xiaotan and Laolin sections the nadir of the excursions occurs in the underlying Daibu Member (Figure 8). The authors speculate that this slight discrepancy may be related to the unique lithology of the members in the Sujiawa section in regards to coeval stratigraphic sections in East Yunnan. The Zhongyicun Member typically contains phosphorites however in nearby sections (see Yang et al., 2016), the base of the Zhongyicun Member is typically

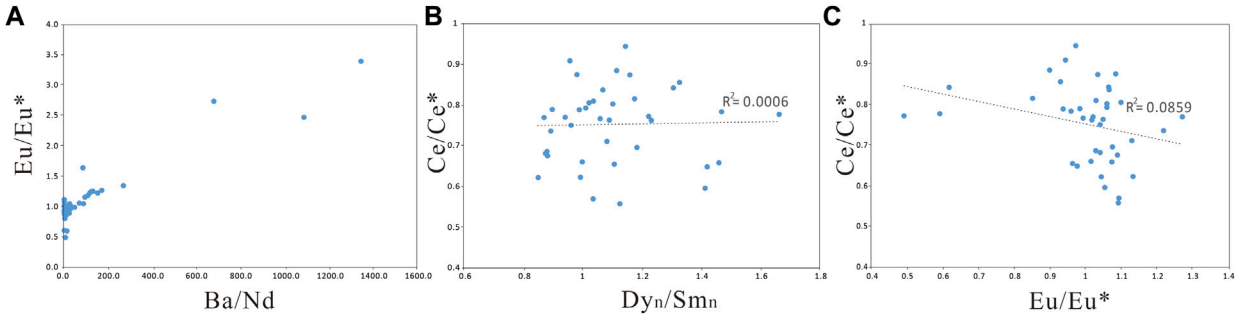

FIGURE 12
(A) Cross plots of Eu anomalies vs. Ba/Nd; **(B)** Ce anomalies vs. Dy_N/Sm_N; **(C)** Ce anomalies vs. Eu anomalies.

defined as silty dolomitic siltstones (Lishuping section) or dark limestone and dolomitic limestone (Laolin section). With this uncertainty in mind, we await robust biostratigraphic controls (the only fossils recovered currently, are indistinct tubular taxa; Figure 7) and numerical age control to assist in the definition of key members and provide additional regional correlation.

5.2.2 Global chemostratigraphic correlation

The current Ediacaran-Cambrian boundary is defined by the first appearance of *T. pedum* and the stratotype section is at Fortune Head in Newfoundland (Figure 3; Brasier et al., 1994; Landing, 1994). The reliability of *T. pedum* as a marker for the base of the Cambrian has been widely criticized (see discussion in Topper et al., 2022) and consequently many studies have turned to alternative proxies to identify the base of the Cambrian in sections worldwide. For example, the first appearance of key shelly fossils (such as *Protohertzina* and *Anabarites*, Figure 3) are frequently utilized as indicators of early Cambrian strata (Kouchinsky et al., 2001; Kouchinsky et al., 2017; Steiner et al., 2007; Steiner et al., 2020; Topper et al., 2022) as is the significant negative carbon excursion (referred to as L1′, N1 or the BACE, Figure 8) that straddles the Ediacaran-Cambrian boundary. Carbon isotope chemostratigraphy has been useful in recognizing the Ediacaran-Cambrian transition in South China (Brasier et al., 1990; Ishikawa et al., 2008; Li et al., 2009; Li et al., 2013; Figures 8B,C), Siberia (Kaufman and Knoll, 1995; Figure 9D; Knoll et al., 1995; Kouchinsky et al., 2001), Mongolia (Braiser et al., 1994; Smith et al., 2016; Yang et al., 2020; Topper et al., 2022; Figure 9B), Iran (Brasier et al., 1990; Kimura et al., 1997), Morocco (Maloof et al., 2010; Figure 9C), and Oman (Amthor et al., 2003). Despite the increasing reliance on carbon isotope chemostratigraphy for regional and international correlation, the accuracy of interpreting carbon isotope curves is somewhat dependent on reliable biostratigraphic data (Betts et al., 2018; Topper et al., 2022). For example, the first appearance of the shelly fossil *Protohertzina* is frequently associated with the prominent negative excursion (the BACE, N1 or L1') and it has been suggested that the shelly taxon could represent an alternative boundary marker to the first appearance of *T. pedum* (Topper et al., 2022). However, in the absence of biostratigraphic markers or radiometric dates, some regions such as Morocco (Maloof et al., 2010) and the Sujiawa section presented herein, must rely predominantly on $\delta^{13}C$ carbon profiles to place the Ediacaran-Cambrian boundary (Maloof et al., 2010).

The chemostratigraphic profile from the Sujiawa section, is here compared with three other $\delta^{13}C$ profiles from Mongolia, Morocco and Siberia (Figure 9). A number of similarities can be drawn and a negative carbon isotope excursion have been reported from each of the four profiles presented. In the Zavkhan Basin in Mongolia, the BACE has been recorded in the upper part of the Zuun-arts Formation (Smith et al., 2016; Topper et al., 2022; Figure 9B). In Morocco's Anti-Atlas Mountains, a negative carbon isotope excursion, "1N" has been documented towards the base of the Tifnout Member (Maloof et al., 2010; Figure 9C) and in Siberia the negative carbon isotope excursion, referred to as "N" as been reported in the Staraya Rechka Formation (Kaufman and Knoll, 1995; Figure 9D). The position and the magnitude of the negative carbon isotope excursion in the Sujiawa section, is comparable to what has been documented from within South China (Figure 8) and the three international sections mentioned above (Figure 9). Like the successions in Morocco, there is not strong biostratigraphic control from the strata in the Sujiawa section, where only tubular fossils have been found. Correlation of the $\delta^{13}C$ profile from the Sujiawa section has been strengthened by similarities to the Laolin and Xiaotan sections where there is some biostratigraphic control.

Based on similar stratigraphic positions, the prominent negative carbon isotope excursion recorded in the Sujiawa section, is most likely the N1 and L1' excursions recorded in the Laolin and Xiaotan sections that have subsequently been correlated with the BACE on a global scale (Li et al., 2009; Li et al., 2013; Topper et al., 2022). With some controversy surrounding at which point of the curve to define the boundary (see Zhu et al., 2019; Topper et al., 2022) we tentatively placed the boundary in the Sujiawa section within the Daibu Member or the Zhongyicun Member awaiting confirmation from biostratigraphic controls.

5.3 Trace elements and redox in the paleoenvironment

5.3.1 Detrital effect and diagenesis

Similar to carbon isotope chemostratigraphy, when rare Earth elements are used in paleoenvironmental studies, it is critical to

ensure that the information extracted from the carbonate rocks is not affected by diagenetic alteration or non-carbonate contaminants. This is because the carbonate leaching processes inevitably erodes (but only partially) the detrital aluminumsilicate components of the samples. The PAAS normalized REE+Y distribution pattern and the carbonate leachate Y/Ho ratio promoted the ability to distinguish the origin of the rare Earth elements signal in the studied samples from seawater. The REE+Y pattern in detrital materials is considered to be relatively flat with a Y/Ho ratio of approximately 28 (Bau et al., 1996). The REE+Y pattern in modern seawater is usually characterized by light REE depletion and negative Ce anomalies with a Y/Ho ratio higher than 60 (Wang et al., 2020).

The lower REE+Y content in the sedimentary rocks from the Sujiawa section than the North American shales composites (NASC) indicates that the material is not contaminated by detritus (200 ppm; Haskin and Gehl, 1962). In addition, if the Y/Ho ratio of sedimentary rocks is higher than that of the North American shales (25.95) and closer to that of modern seawater (45), it similarly indicates the presence of small amounts of terrigenous detritus in the rock samples (Webb and Kamber, 2000). The REE+Y contents of the strata in the Sujiawa section are basically <200 ppm (Supplementary Table S2). The Y/Ho ratios range from 28.0 to 64.9 (Supplementary Table S2), with the majority of samples having a much higher Y/Ho ratios than the North American shales. This suggests that the REE+Y signal in these samples is mainly from seawater rather than detrital materials. In addition, comparing Y/Ho to the abundance of elements found in oxides and sulfides can be used to determine if carbonate rocks are contaminated with non-carbonate minerals, including Ni (which indicates oxide enrichment) and Sc (which indicates sulfide enrichment). The Ni and Sc content of the carbonate rocks in this study is low. As seen in Figure 10, Ni does not correlate with Y/Ho values, indicating the absence of oxide contaminants in the leachate. In addition, the lack of correlation between Sc and Y/Ho indicates that these samples have not been contaminated with sulfides (Wang et al., 2020). Overall, these results suggest that the leachate of these samples are not contaminated with debris and consequently the REE+Y values can reflect the palaeo-redox conditions more accurately.

Previous studies (Webb and Kamber, 2000; Nothdurft et al., 2004; Ling et al., 2013) have demonstrated that REE data for samples with Al < 0.30%, Fe < 0.45%, Th < 0.30 ppm, Sc < 2 ppm, REE <10 ppm, and Y/Ho > 36 are environmentally significant. In this study, there may be differences in total rare Earth elements for samples that do not meet the above criteria, but the shale normalized delineation pattern and main parameter characteristics are the same (Figure 11) and can be utilized in the interpretation of sedimentary environmental traceability. Here the Eu anomalies in Supplementary Table S2 were calculated using $Eu/Eu^{*}= Eu_N/(Sm_N^2 \times Tb_N)^{1/3}$ (Lawrence et al., 2006). The majority of samples through the Sujiawa section show positive Eu anomalies (>1). Positive Eu anomalies can be caused by hydrothermal fluid or interference by various barium compounds when measured by ICP-MS (Dulski, 1994). Such artificially positive Eu anomalies can be detected by positive correlation between Ba/Nd and Eu/Eu* (Ling et al., 2013). Most of the samples from the Sujiawa section, including the Baiyanshao Member, Daibu Member and Zhongyicun Member, have high Ba/Nd (>20) and show positive correlation between Eu/Eu* and Ba/Nd (Supplementary Table S2; Figure 12). This suggests that ICP-MS measurement errors caused by Ba may have contributed to the artificially positive Eu anomalies. However, except for the samples with Ba/Nd > 20, the Eu positive anomalies of the remaining samples from the Sujiawa section are small and comparable to previous studies (Slack et al., 2007; Ling et al., 2013). In this case, the contribution of Ce derived from hydrothermal fluids is negligible (<1%) (Slack et al., 2007).

Although REE is generally stable during carbonate diagenesis (Webb et al., 2009), diagenesis can cause REE patterns to push towards more Ce enrichment, Eu loss and low Dy_N/Sm_N, thus showing a negative correlation between Ce/Ce* and Eu/Eu* and Dy_N/Sm_N (Shields and Stille, 2001). For interpreting diagenesis of Ce anomalies, we excluded the samples with high Ba/Nd (>20), and drew cross-plots of Ce/Ce* vs. Eu/Eu* and Ce/Ce* vs. Dy_N/Sm_N. No negative correlation between them was detected (Figure 12). This suggests that the Ce anomalies were not altered by hydrothermal fluid or diagenesis.

5.3.2 Ce anomaly

Trace element and REE distributions in marine carbonates are considered representative of trace element and REE distributions in seawater at the time of deposition (Zhao and Zheng, 2014; Liu et al., 2019). As such, trace elements and REE can provide evidence regarding the depositional environment of the carbonate formation (Ling et al., 2013; Wei et al., 2018).

In oxidized seawater, Ce^{3+} is easily oxidized to insoluble Ce^{4+}, which is more easily adsorbed onto particles and separates from other REEs, resulting in negative Ce anomalies in seawater. In anoxic seawater, the extent of negative Ce anomalies is reduced or even absent (Guo et al., 2007). Because of this, Ce anomalies have been frequently used to determine redox environments (Ling et al., 2013; Wei et al., 2018; Wang et al., 2020). Ce/Ce* data after strict screening (Figure 4; Supplementary Table S2) infers that the Ce profile in the Sujiawa section reflects the paleo-redox environment of the Ediacaran-Cambrian in East Yunnan. The dolomite in the lower part of the Baiyanshao Member of the Dengying Formation in the Sujiawa section was deposited in a suboxic environment and the limestone in the upper part in a suboxic-oxic environment. The Daibu Member of the Zhujiaqing Formation represents an oxic-suboxic environment and the lower part of the Zhongyicun Member was deposited in an anoxic environment, with the upper part of the member indicating deposition in an anoxic environment-suboxic environment. We can see that across the E-C transition, there are noticeable changes in the paleo-redox environment. From the Baiyanshao Member to the lower part of Daibu Member, the paleo-redox environment is in a partially oxidizing environment, this changes at the top of the Daibu Member and the bottom of the Zhongyicun Member (the nadir of the prominent negative excursion) where the paleo-redox environment changes from suboxic to anoxic, and this change is consistent with the trend of previous studies (Ling et al., 2013). Towards the middle of the Zhongyicun Member, the palaeo-redox environment changes again to a suboxic environment, and the top of the Zhongyicun Member, represents an anoxic reduction environment.

5.3.3 Paleoenviroment during the E-C transition

Reconstruction of paleoenvironments during the Ediacaran-Cambrian transition is crucial for understanding the "Cambrian

Explosion". As one of the most characteristic geochemical signatures across the E-C boundary, the significant negative carbon isotope excursion provides important clues for understanding what happened during this interval. Numerous mechanisms have been proposed to explain the geochemical and biological changes, including severe methane release (Kirschvink and Raub, 2003), oceanic anoxia (Kimura and Watanabe, 2001), hydrothermal activities (Steiner et al., 2001), termination of an unusually large oceanic reservoir of organic carbon (Rothman et al., 2003) and upwelling of euxinic bottom waters (Wille et al., 2008).

The absolute values of the BACE (N1 and L1') vary significantly in carbonate sections around the globe. In South China, the absolute values of the N1 excursion in the Xiaotan section is −12.2‰ (Li et al., 2013), whereas the L1' in the Laolin section is −7.2‰ (Li et al., 2009) and in the Sujiawa section the negative carbon isotope excursion reaches −7.3‰. These values are comparable to other sections around the world, that show a similar range of absolute $\delta^{13}C_{carb}$ values. For example, in Mongolia the BACE reaches −10.2‰ (Topper et al., 2022), whereas in Morocco, absolute values only reach −5.2‰ (Maloof et al., 2010). Many reasons have been put forth to explain large differences in absolute $\delta^{13}C_{carb}$ values. Paleobathymetry has been suggested to play a role in absolute $\delta^{13}C_{carb}$ values as the surface water has $\delta^{13}C_{carb}$ values that are heavier by about 2‰–3‰ than deep water values in modern oceans (e.g., Kroopnick, 1985; Gruber et al., 1999; Sarmiento and Gruber, 2006). This vertical gradient is due to an increase biological activity (Raven and Falkowski, 1999), as photosynthesis in the oceans is limited to the photic zone, causing depletion in ^{12}C in the surface water. Absolute $\delta^{13}C_{carb}$ values can also be affected by diagenetic alteration (e.g., Derry et al., 1992). However, we have shown here using rare Earth element analyses that the Sujiawa section has undergone limited diagenesis, so it is likely that diagenesis has not played a significant role in the isotopic signal in the Sujiawa section. Mineralogy has also been utilized to explain differences in absolute $\delta^{13}C_{carb}$ values, as limestone samples can have marginally higher $\delta^{13}C_{carb}$ values than dolostone (Pulsipher et al., 2021). It has also been shown that paleogeography can affect absolute values, as $\delta^{13}C_{carb}$ values in surface waters at high latitudes (colder) is higher with respect to the atmosphere than in the warmer, low latitude ocean surface waters by ~ 2‰ (Lynch Stieglitz et al., 1995; Lynch-Stieglitz, 2003). These values contrast with warmer water temperatures in low latitudes that may result in higher levels of primary productivity resulting in higher $\delta^{13}C_{carb}$ values (Hollander and McKenzie, 1991; Pulsipher et al., 2021). Finally, the presence of organic matter also potentially plays a significant role in determining absolute $\delta^{13}C_{carb}$ values, as preservation of organic matter under anoxic or euxinic conditions together with terrigenous organic matter input (Lehmann et al., 2002; Izumi et al., 2012; Li et al., 2020) can cause negative carbon isotope excursions. The Sujiawa section shows a relatively lower value of negative carbon isotope when compared to sections such as Xiaotan and the BAY4/5 section in Mongolia (Li et al., 2013; Topper et al., 2022). The Sujiawa section was near the equator (11–18°S), deposited in a slightly deeper water setting (when compared with other sections in South China) and the excursion coincided with anoxic conditions (as shown by Ce anomalies), which may have limited biological activity at the time. The nadir of the carbon isotope excursion in the Sujiawa section was also recorded in black phosphorite dolostone that represents increased organic content (Qian et al., 1996; Zhu et al., 2007). Based on the evidence presented in this paper and the potential mechanisms mentioned above, the lower absolute $\delta^{13}C_{carb}$ values observed in the Sujiawa section (when compared to select sections worldwide) may have been caused by a combination of paleobathymetry, paleogeography, mineralogy, anoxia and the presence of increased organic content.

In the Sujiawa section, positive Ce anomalies during the E-C transition suggest that the paleoenvironment was in anoxic conditions (Figure 4). Many scholars have presented evidence of anoxia around the E-C transition (Ling et al., 2013; Jin et al., 2016; Sahoo et al., 2016; Wei et al., 2018; Wood and Erwin, 2018; Wood et al., 2019; Wang et al., 2020). For example, some previous studies in Oman (Schroder and Grotzinger, 2007) and Anhui, China (Chang et al., 2017) have reported enriched V (Vanadium) and U (Uranium) in black shales near the Ediacaran-Cambrian boundary representing deposition in anoxic environments ((Oman's black shale age is 542.0 ± 0.3 Ma (Amthor et al., 2003), the stratigraphic age of Re-Os isotope analysis in South China is 541 ± 16 Ma (Mao et al., 2002)). To explain these periods of shallow sea anoxia in the E-C transition, a number of mechanisms have been proposed. These include, increased particulate organic carbon produced by plankton (Rothman et al., 2003), upwelling of euxinic bottom waters (Wille et al., 2008; Chang et al., 2017), and transgressive events (Zhu et al., 2004). It has been previously suggested that transgressive events and the upwelling of euxinic bottom waters may have been a driving force behind anoxic conditions at this time (Zhu et al., 2004; Dilliard et al., 2007; Guo et al., 2010; Wang et al., 2011). The frequent juxtaposition of anoxic conditions and negative carbon isotope excursions in the vicinity of the Ediacaran-Cambrian boundary suggests that there may be a link between the two phenomena. Whether there is a direct link between negative carbon isotope excursions and anoxia will rely on future studies, but it will be crucial in our understanding of the environmental conditions that witnessed the evolution and diversification of the earliest animals.

6 Conclusion

(1) The Sujiawa section preserves a thick, continuous, predominantly carbonate sequence through Ediacaran-Cambrian strata in East Yunnan. A prominent negative carbon isotope excursion occurs in what is interpreted as the basal Zhongyicun Member, most likely represents the negative carbon excursion reported in many localities across the Ediacaran-Cambrian transition (BACE, N1, L1′). This suggests that the Ediacaran-Cambrian boundary should be placed in the proximity of the Daibu and Zhongyicun members of the Sujiawa section awaiting further information from diagnostic shelly fossils or radiometric dates.

(2) The Ce anomalies in the Sujiawa section reflects paleoenviroment changes from oxic to anoxic conditions during the Ediacaran-Cambrian transition. Therefore, we speculate that shallow sea anoxic events that occur during

the Ediacaran-Cambrian transition may be related to the prominent negative carbon excursion that has been recorded across the globe (BACE, N1 and L1′).

Data availability statement

The original contributions presented in the study are included in the article/Supplementary material, further inquiries can be directed to the corresponding author.

Author contributions

YC conceived the project, XY undertook data analysis and led the writing of the manuscript. ZZ supervised all the field works and section-selecting and came up with the hypothesis and provided financial support for the project. CC and YC led chemical analysis and interpretation of stratigraphy. TT provided discussion and assisted with revising and polishing the manuscript. FL and YL participated in all aspects of the fieldwork and provided an internal review of the manuscript. RF provided fossils and participated in the fieldwork. All authors contributed to the article and approved the submitted version.

Funding

The present research was supported by the National Nature Science Foundation of China (NSFC 41890844, 41720104002, 42172013, 41425008, 41621003, 42072003, and 42272006), and by 111 Project (D17013). ZZ acknowledges the Changjiang Scholars (T2016155 to ZZ), Department of science and technology of Shaanxi Province (2022TD-11) and Wanrenjihua programmes (W03020685 to ZZ) for continuous supports for his laboratory and field works. TT acknowledges the Swedish Research Council (grants VR 2016-04610 and VR 2021-04295).

Acknowledgments

Thanks to Zhai Juanping, Zhang Qian, Fu Rao, Song Baopeng, Luo Mei, Wang Jiayue, Zhang Caibin, Wang Zhao for their generous help in fieldwork and sample collection, Wang Zhenfei and Li Yining for their experimental help in carbon isotope analyses, and Hu Yang for their experimental helps in major and trace elements analyses.

Conflict of interest

The authors declare that the research was conducted in the absence of any commercial or financial relationships that could be construed as a potential conflict of interest.

Publisher's note

Supplementary Material

The Supplementary Material for this article can be found online at: https://www.frontiersin.org/articles/10.3389/feart.2023.1173846/full#supplementary-material

References

Amthor, J. E., Grotzinger, J. P., Schroder, S., Bowring, S. A., Ramezani, J., Martin, M. W., et al. (2003). Extinction of Cloudina and namacalathus at the precambrian - cambrian boundary in Oman. *Geology* 5, 431–434. doi:10.1130/0091-7613(2003)031<0431:EOCANA>2.0.CO;2

Azmy, K., Brand, U., Sylvester, P., Gleeson, S. A., Logan, A., and Bitner, M. A. (2011). Biogenic and abiogenic low-Mg calcite (bLMC and aLMC): Evaluation of seawater-REE composition, water masses and carbonate diagenesis. *Chem. Geol.* 280 (1-2), 180–190. doi:10.1016/j.chemgeo.2010.11.007

Azmy, K., Stouge, S., Brand, U., Bagnoli, G., and Ripperdan, R. (2014). High-resolution chemostratigraphy of the cambrian–ordovician GSSP: Enhanced global correlation tool. *Palaeogeogr. Palaeocl* 409, 135–144. doi:10.1016/j.palaeo.2014.05.010

Babcock, L. E., Peng, S., Zhu, M., Xiao, S., and Ahlberg, P. (2014). Proposed reassessment of the cambrian gssp. *J. Afr. Earth Sci.* 98, 3–10. doi:10.1016/j.jafrearsci.2014.06.023

Bartley, J. K., Pope, M., Knoll, A. H., Semikhatov, M. A., and Petrov, P. Y. (1998). A Vendian–Cambrian boundary succession from the northwestern margin of the Siberian Platform; stratigraphy, palaeontology, chemostratigraphy and correlation. *Geol. Mag.* 135, 473–494. doi:10.1017/S0016756898008772

Bathurst, R. G. C. (1975). "Carbonate sediments and their diagenesis," in *Development in Sedimentology* (Amsterdam: Elsevier), 1–658.

Bau, M., Koschinsky, A., Dulski, P., and Hein, J. R. (1996). Comparison of the partitioning behaviours of yttrium, rare Earth elements, and titanium between hydrogenetic marine ferromanganese crusts and seawater. *Geochim. Cosmochim. Ac* 60, 1709–1725. doi:10.1016/0016-7037(96)00063-4

Betts, M. J., Paterson, J. R., Jacquet, S. M., Andrew, A. S., Hall, P. A., Jago, J. B., et al. (2018). Early cambrian chronostratigraphy and geochronology of SouthSouth Australia. *Earth-Sci Rev.* 185, 498–543. doi:10.1016/j.earscirev.2018.06.005

Bowyer, F. T., Zhuravlev, A. Y., Wood, R., Shields, G. A., Zhou, Y., Curtis, A., et al. (2022). Calibrating the temporal and spatial dynamics of the Ediacaran-Cambrian radiation of animals. *Earth-Sci Rev.* 225, 103913. doi:10.1016/j.earscirev.2021.103913

Bowyer, F. T., Zhuravlev, A. Y., Wood, R., Zhao, F., Sukhov, S. S., Alexander, R. D., et al. (2023). Implications of an integrated late ediacaran to early cambrian stratigraphy of the siberian platform, Russia. *Geol. Soc. Am. Bull.* doi:10.1130/B36534.1

Brand, U., and Veizer, J. (1980). Chemical diagenesis of a multicomponent carbonate system; 1, Trace elements. *J. Sedimen*t. Res. 50 (4), 1219–1236. doi:10.1306/212F7BB7-2B24-11D7-8648000102C1865D

Brasier, M. D., Corfield, R. M., Derry, L. A., Rozanov, A. Y., and Zhuravlev, A. Y. (1994). Multiple $\delta^{13}C$ excursions spanning the Cambrian explosion to the Botomian crisis in Siberia. *Geology* 22 (5), 455–458. doi:10.1130/0091-7613(1994022)<0455:MCESTC>2.3.CO;2

Brasier, M. D., Magaritz, M., Corfield, R., Luo, H., Wu, X., Ouyang, L., et al. (1990). The carbon- and oxygen-isotope record of the Precambrian–Cambrian boundary interval in China and Iran and their correlation. *Geol. Mag.* 127, 319–332. doi:10.1017/S0016756800014886

Buatois, L. A. (2018). Treptichnus pedum and the Ediacaran–Cambrian boundary: significance and caveats. *Geol. Mag.* 155 (1), 174–180. doi:10.1017/S0016756817000656

Budd, G. E. (2003). The Cambrian fossil record and the origin of the phyla.*Integr. Comp. Biol.* 43 (1), 58–70. doi:10.1093/icb/43.1.157

Cai, Y., Xiao, S., Li, G., and Hua, H. (2019). Diverse biomineralizing animals in the terminal Ediacaran Period herald the Cambrian explosion. *Geol.* 47 (4), 380–384. doi:10.1130/G45949.1

Chang, C., Hu, W., Wang, X., Yao, S., Yang, A., Cao, J., et al. (2017). Carbon isotope stratigraphy of the lower to middle Cambrian on the eastern Yangtze Platform, South China. *Palaeogeogr. Palaeocl* 479, 90–101. doi:10.1016/j.palaeo.2017.04.019

Chen, L, Z., Luo, H, L., and Hu, S, X. (2002). Early cambrian chengjiang fauna in East Yunnan, China. *Yunnan Geo* 22 (2), 1. doi:10.3969/j.issn.1004-1885.2003.02.014

Cherry, L. B., Gilleaudeau, G. J., Grazhdankin, D. V., Romaniello, S. J., Martin, A. J., and Kaufman, A. J. (2022). A diverse Ediacara assemblage survived under low-oxygen conditions. *Nat. Commun.* 13 (1), 7306–7311. doi:10.1038/S41467-022-35012-Y

Darroch, S. A., Smith, E. F., Laflamme, M., and Erwin, D. H. (2018). Ediacaran extinction and Cambrian explosion. *Trends Eco Evo* 33 (9), 653–663. doi:10.1016/j.tree.2018.06.003

Derry, L. A., Brasier, M. D., Corfield, R. E. A., Rozanov, A. Y., and Zhuravlev, A. Y. (1994). Sr and C isotopes in lower cambrian carbonates from the siberian craton: A paleoenvironmental record during the 'cambrian explosion. *Earth Planet S. C. Lett.* 128 (3-4), 671–681. doi:10.1016/0012-821X(94)90178-3

Derry, L. A., Kaufman, A. J., and Jacobsen, S. B. (1992). Sedimentary cycling and environmental change in the late proterozoic: Evidence from stable and radiogenic isotopes. *Geochim. Cosmochim. Ac* 56 (3), 1317–1329. doi:10.1016/0016-7037(92)90064-P

Dilliard, K. A., Pope, M. C., Coniglio, M., Hasiotis, S. T., and Lieberman, B. S. (2007). Stable isotope geochemistry of the lower Cambrian Sekwi Formation, Northwest Territories, Canada: Implications for ocean chemistry and secular curve generation. *Palaeogeogr. Palaeocl* 256, 174–194. doi:10.1016/j.palaeo.2007.02.031

Dulski, P. (1994). Interferences of oxide, hydroxide and chloride analyte species in the determination of rare Earth elements in geological samples by inductively coupled plasma-mass spectrometry. *Fresenius' J. Anal. Chem.* 350, 194–203. doi:10.1007/BF00322470

Gehling, J. G., JENSEN, S., Droser, M. L., Myrow, P. M., and Narbonne, G. M. (2001). Burrowing below the basal Cambrian GSSP, fortune head, Newfoundland. *Geol. Mag.* 138 (2), 213–218. doi:10.1017/s001675680100509x

Geyer, G. (2005). The Fish River Subgroup in Namibia: stratigraphy, depositional environments and the Proterozoic–Cambrian boundary problem revisited. *Geol. Mag.* 142 (5), 465–498. doi:10.1017/S0016756805000956

Geyer, G. (2019). A comprehensive Cambrian correlation chart. *Episodes J. Int. Geoscience* 42 (4), 321–332.

Grotzinger, J. P., Bowring, S. A., Saylor, B. Z., and Kaufman, A. J. (1995). Biostratigraphic and geochronologic constraints on early animal evolution. *Science* 270 (5236), 598–604. doi:10.1126/science.270.5236.598

Gruber, N., Keeling, C. D., Bacastow, R. B., Guenther, P. R., Lueker, T. J., Wahlen, M., et al. (1999). Spatiotemporal patterns of carbon-13 in the global surface oceans and the oceanic Suess effect. *Glob. Biogeochem. cycles* 13 (2), 307–335. doi:10.1029/1999GB900019

Guo, Q., Shields, G. A., Liu, C., Strauss, H., Zhu, M., Pi, D., et al. (2007). Trace element chemostratigraphy of two ediacaran–cambrian successions in SouthSouth China: Implications for organosedimentary metal enrichment and silicification in the early cambrian. *Palaeogeogr. Palaeocl* 254 (1-2), 194–216. doi:10.1016/j.palaeo.2007.03.016

Guo, Q., Strauss, H., Liu, C., Zhao, Y., Yang, X., Peng, J., et al. (2010). A negative carbon isotope excursion defines the boundary from cambrian series 2 to cambrian series 3 on the Yangtze platform, South China. *Palaeogeogr. Palaeocl* 288, 143–151. doi:10.1016/j.palaeo.2009.11.005

Haskin, L., and Gehl, M. A. (1962). The rare-Earth distribution in sediments. *J. Geophys Res.* 67 (6), 2537–2541. doi:10.1029/jz067i006p02537

Hollander, D. J., and McKenzie, J. A. (1991). CO2 control on carbon-isotope fractionation during aqueous photosynthesis: A paleo-pCO2 barometer. *Geology* 19 (9), 929–932. doi:10.1130/0091-7613(1991)019<0929:CCOCIF>2.3.CO;2

Ishikawa, T., Ueno, Y., Komiya, T., Sawaki, Y., Han, J., Shu, D., et al. (2008). Carbon isotope chemostratigraphy of a precambrian/cambrian boundary section in the three gorge area, South China: Prominent global-scale isotope excursions just before the cambrian explosion. *Gondwana Res.* 14 (1-2), 193–208. doi:10.1016/j.gr.2007.10.008

Ishikawa, T., Ueno, Y., Shu, D., Li, Y., Han, J., Guo, J., et al. (2014). The $\delta^{13}C$ excursions spanning the Cambrian explosion to the Canglangpuian mass extinction in the Three Gorges area, South China. *Gondwana Res.* 25 (3), 1045–1056. doi:10.1016/j.gr.2013.03.010

Izumi, K., Miyaji, T., and Tanabe, K. (2012). Early Toarcian (Early Jurassic) oceanic anoxic event recorded in the shelf deposits in the northwestern Panthalassa: Evidence from the Nishinakayama Formation in the Toyora area, west Japan. *Palaeogeogr. Palaeoclimatol. Palaeoecol.* 315, 100–108. doi:10.1016/j.palaeo.2011.11.016

Jiang, G., Wang, X., Shi, X., Xiao, S., Zhang, S., and Dong, J. (2012). The origin of decoupled carbonate and organic carbon isotope signatures in the early Cambrian (ca 542–520 Ma) Yangtze platform. *Earth Planet S. C. Lett.* 317, 96–110. doi:10.1016/j.epsl.2011.11.018

Jin, C., Li, C., Algeo, T. J., Planavsky, N. J., Cui, H., Yang, X., et al. (2016). A highly redox-heterogeneous ocean in South China during the early Cambrian (529–514 Ma): Implications for biota-environment co-evolution. *Earth Planet S. C. Lett.* 441, 38–51. doi:10.1016/j.epsl.2016.02.019

Kaufman, A. J., and Knoll, A. H. (1995). Neoproterozoic variations in the C-isotopic composition of seawater: Stratigraphic and biogeochemical implications. *Precambrian Res.* 73 (1-4), 27–49. doi:10.1016/0301-9268(94)00070-8

Kimura, H., Matsumoto, R., Kakuwa, Y., Hamdi, B., and Zibaseresht, H. (1997). The vendian-cambrian $\delta^{13}C$ record, North Iran: Evidence for overturning of the ocean before the cambrian explosion. *Earth Planet S. C. Lett.* 147 (1-4), E1–E7. doi:10.1016/S0012-821X(97)00014-9

Kimura, H., and Watanabe, Y. (2001). Oceanic anoxia at the Precambrian-Cambrian boundary. *Geology* 29 (11), 995–998. doi:10.1130/0091-7613(2001)029<0995:OAATPC>2.0.CO;2

Kirschvink, J. L., and Raub, T. D. (2003). A methane fuse for the Cambrian explosion: carbon cycles and true polar wander. *Cr Geosci.* 335 (1), 65–78. doi:10.1016/S1631-0713(03)00011-7

Knoll, A. H., Kaufman, A. J., Semikhatov, M. A., and Adams, W. (1995). Sizing up the sub-Tommotian unconformity in Siberia. *Geology* 23, 1139–1143. doi:10.1130/0091-7613(1995)023<1139:SUTSTU>2.3.CO;2

Knoll, A. H., and Carroll, S. B. (1999). Early animal evolution: Emerging views from comparative biology and geology. *Science* 284 (5423), 2129–2137. doi:10.1126/science.284.5423.2129

Komiya, T., Hirata, T., Kitajima, K., Yamamoto, S., Shibuya, T., Sawaki, Y., et al. (2008). Evolution of the composition of seawater through geologic time, and its influence on the evolution of life. *Gondwana Res.* 14 (1-2), 159–174. doi:10.1016/j.gr.2007.10.006

Kouchinsky, A., Bengtson, S., Missarzhevsky, V. V., Pelechaty, S., Torssander, P., and Val'Kov, A. K. (2001). Carbon isotope stratigraphy and the problem of a pre-Tommotian Stage in Siberia. *Geol. Mag.* 138 (4), 387–396. doi:10.1017/s0016756801005684

Kouchinsky, A., Bengtson, S., Landing, E., Steiner, M., Vendrasco, M., and Ziegler, K. (2017). Terreneuvian stratigraphy and faunas from the Anabar Uplift, Siberia. *Acta Palaeonto Pol.* 62 (2), 311–440. doi:10.4202/app.00289.2016

Kroopnick, P. M. (1985). The distribution of 13C of ΣCO2 in the world oceans. *Deep Sea Res. Part A. Oceanogr. Res. Pap.* 32 (1), 57–84. doi:10.1016/0198-0149(85)90017-2

Landing, E., Geyer, G., Brasier, M. D., and Bowring, S. A. (2013). Cambrian evolutionary radiation: context, correlation, and chronostratigraphy—overcoming deficiencies of the first appearance datum (FAD) concept. *Earth Sci. Rev.* 123, 133–172. doi:10.1016/j.earscirev.2013.03.008

Landing, E. (1994). Precambrian-Cambrian boundary global stratotype ratified and a new perspective of Cambrian time. *Geology* 22 (2), 179–182. doi:10.1130/0091-7613(1994)022<0179:PCBGSR>2.3.CO;2

Lawrence, M. G., Greig, A., Collerson, K. D., and Kamber, B. S. (2006). Rare Earth element and yttrium variability in South East Queensland waterways. *Aquat. Geochem* 12, 39–72. doi:10.1007/s10498-005-4471-8

Lehmann, M. F., Bernasconi, S. M., Barbieri, A., and McKenzie, J. A. (2002). Preservation of organic matter and alteration of its carbon and nitrogen isotope composition during simulated and *in situ* early sedimentary diagenesis. *Geochimica Cosmochimica Acta* 66 (20), 3573–3584. doi:10.1016/S0016-7037(02)00968-7

Li, D. A., Ling, H. F., Jiang, S. Y., Pan, J. Y., Chen, Y. Q., Cai, Y. F., et al. (2009). New carbon isotope stratigraphy of the ediacaran–cambrian boundary interval from SW China: Implications for global correlation. *Geol. Mag.* 146 (4), 465–484. doi:10.1017/S0016756809006268

Li, D., Ling, H. F., Shields-Zhou, G. A., Chen, X., Cremonese, L., Och, L., et al. (2013). Carbon and strontium isotope evolution of seawater across the ediacaran–cambrian transition: Evidence from the xiaotan section, NE yunnan, South China. *Precambrian Res.* 225, 128–147. doi:10.1016/j.precamres.2012.01.002

Li, G., Zhang, J., and Zhu, M. (2001). Litho- and biostratigraphy of the lower cambrian meishucunian stage in the xiaotan section, eastern yunnan. *Acta Palaeont sin.* 40, 40–53.

Li, L., Liao, Z., Lei, L., Lash, G. G., Chen, A., and Tan, X. (2020). On the negative carbon isotope excursion across the wuchiapingian–changhsingian transition: A regional event in the lower Yangtze region, South China? *Palaeogeogr. Palaeoclimatol. Palaeoecol.* 540, 109501. doi:10.1016/j.palaeo.2019.109501

Ling, H. F., Chen, X., Li, D. A., Wang, D., Shields-Zhou, G. A., and Zhu, M. (2013). Cerium anomaly variations in ediacaran–earliest cambrian carbonates from the Yangtze gorges area, South China: Implications for oxygenation of coeval shallow seawater. *Precambrian Res.* 225, 110–127. doi:10.1016/j.precamres.2011.10.011

Liu, X. M., Hardisty, D. S., Lyons, T. W., and Swart, P. K. (2019). Evaluating the fidelity of the cerium paleoredox tracer during variable carbonate diagenesis on the Great Bahamas Bank. *Geochim. Cosmochim. Ac* 248, 25–42. doi:10.1016/j.gca.2018.12.028

Luo, H., Jiang, Z., Wu, X., Song, X., and Ouyang, L. (1982). *The sinian–cambrian boundary in eastern yunnan*. Kunming: Yunnan People's Publishing.

Lynch-Stieglitz, J. (2003). Tracers of past ocean circulation. *Treatise Geochem.* 6, 433–451. doi:10.1016/B0-08-043751-6/06117-X

Lynch-Stieglitz, J., Stocker, T. F., Broecker, W. S., and Fairbanks, R. G. (1995). The influence of air-sea exchange on the isotopic composition of oceanic carbon: Observations and modeling. *Glob. Biogeochem. Cycles* 9 (4), 653–665. doi:10.1029/95GB02574

Maloof, A. C., Porter, S. M., Moore, J. L., Dudás, F. Ö., Bowring, S. A., Higgins, J. A., et al. (2010). The earliest Cambrian record of animals and ocean geochemical change. *GSA Bull.* 122 (11-12), 1731–1774. doi:10.1130/B30346.1

Mao, J., Lehmann, B., Du, A., Zhang, G., Ma, D., Wang, Y., et al. (2002). Re-Os dating of polymetallic Ni-Mo-PGE-Au mineralization in Lower Cambrian black shales of South China and its geologic significance. *Econ. Geol.* 97 (5), 1051–1061. doi:10.2113/gsecongeo.97.5.1051

Marshall, C. R. (2006). Explaining the Cambrian "explosion" of animals. *Annu. Rev. Earth Planet Sci.* 34, 355–384. doi:10.1146/annurev.earth.33.031504.103001

Muscente, A. D., Bykova, N., Boag, T. H., Buatois, L. A., Mángano, M. G., Eleish, A., et al. (2019). Ediacaran biozones identified with network analysis provide evidence for pulsed extinctions of early complex life. *Nat. Commun.* 10 (1), 911–915. doi:10.1038/s41467-019-08837-3

Nothdurft, L. D., Webb, G. E., and Kamber, B. S. (2004). Rare earth element geochemistry of Late Devonian reefal carbonates, Canning Basin, Western Australia: confirmation of a seawater REE proxy in ancient limestones. *Geochim Cosmochim Ac.* 68 (2), 263–283. doi:10.1016/S0016-7037(03)00422-8

Peng, S. C., and Babcock, L. E. (2011). Continuing progress on chronostratigraphic subdivision of the Cambrian System. *B Geosci.* 86 (3), 391–396. doi:10.3140/bull.geosci.1273

Pulsipher, M. A., Schiffbauer, J. D., Jeffrey, M. J., Huntley, J. W., Fike, D. A., and Shelton, K. L. (2021). A meta-analysis of the steptoean positive carbon isotope excursion: The SPICEraq database. *Earth-Science Rev.* 212, 103442. doi:10.1016/j.earscirev.2020.103442

Qian, Y., Zhu, M., He, T., and Jiang, Z. (1996). New investigation of Precambrian–Cambrian boundary sections in eastern Yunnan. *Acta Micropalaeontologica Sin.* 13, 225–240.

Qian, Y., Zhu, M. Y., Li, G. X., Jiang, Z. W., and Van Iten, H. (2002). A supplemental Precambrian-Cambrian boundary global stratotype section in SW China. *Acta Palaeont Sin.* 41 (1), 19–26.

Raven, J. A., and Falkowski, P. G. (1999). Oceanic sinks for atmospheric CO2. *Plant, Cell. and Environ.* 22 (6), 741–755. doi:10.1046/j.1365-3040.1999.00419.x

Rothman, D. H., Hayes, J. M., and Summons, R. E. (2003). Dynamics of the Neoproterozoic carbon cycle. *P Natl. A Sci.* 100 (14), 8124–8129. doi:10.1073/PNAS.0832439100

Rozanov, A. Y. (1967). The Cambrian lower boundary problem. *Geol. Mag.* 104 (5), 415–434. doi:10.1017/S0016756800049165

Sahoo, S. K., Planavsky, N. J., Jiang, G., Kendall, B., Owens, J. D., Wang, X., et al. (2016). Oceanic oxygenation events in the anoxic Ediacaran ocean. *Geobiology* 5, 457–468. doi:10.1111/gbi.12182

Sarmiento, J. L., and Gruber, N. (2006). *Ocean biogeochemical dynamics*. USA: Princeton university press, 503. doi:10.1515/9781400849079

Schroder, S., and Grotzinger, J. P. (2007). Evidence for anoxia at the ediacaran–cambrian boundary: The record of redox-sensitive trace elements and rare Earth elements in Oman. *J. Geol. Soc.* 164 (1), 175–187. doi:10.1144/0016-76492005-022

Shahkarami, S., Buatois, L. A., Mángano, M. G., Hagadorn, J. W., and Almond, J. (2020). The ediacaran–cambrian boundary: Evaluating stratigraphic completeness and the great unconformity. *Precambrian Res.* 345, 105721. doi:10.1016/j.precamres.2020.105721

Shen, Y., and Schidlowski, M. (2000). New C isotope stratigraphy from southwest China: Implications for the placement of the Precambrian-Cambrian boundary on the Yangtze Platform and global correlations. *Geology* 28 (7), 623–626. doi:10.1130/0091-7613(2000)28<623:NCISFS>2.0.CO;2

Shields, G., and Stille, P. (2001). Diagenetic constraints on the use of cerium anomalies as palaeoseawater redox proxies: An isotopic and REE study of cambrian phosphorites. *Chem. Geol.* 175 (1-2), 29–48. doi:10.1016/S0009-2541(00)00362-4

Slack, J. F., Grenne, T., Bekker, A., Rouxel, O. J., and Lindberg, P. A. (2007). Suboxic deep seawater in the late paleoproterozoic: Evidence from hematitic chert and iron formation related to seafloor-hydrothermal sulfide deposits, central Arizona, USA. *Earth Planet Sci. Lett.* 255 (1-2), 243–256. doi:10.1016/j.epsl.2006.12.018

Smith, E. F., Macdonald, F. A., Petach, T. A., Bold, U., and Schrag, D. P. (2016). Integrated stratigraphic, geochemical, and paleontological late Ediacaran to early Cambrian records from southwestern Mongolia. *Bulletin* 128 (3-4), 442–468. doi:10.1130/b31248.1

Steiner, M., Li, G., Qian, Y., Zhu, M., and Erdtmann, B. D. (2007). Neoproterozoic to early Cambrian small shelly fossil assemblages and a revised biostratigraphic correlation of the Yangtze Platform (China). *Palaeogeogr. Palaeocl* 254 (1-2), 67–99. doi:10.1016/j.palaeo.2007.03.046

Steiner, M., Wallis, E., Erdtmann, B. D., Zhao, Y., and Yang, R. (2001). Submarine-hydrothermal exhalative ore layers in black shales from South China and associated fossils—Insights into a lower cambrian facies and bio– evolution. *Palaeogeogr. Palaeocl* 169 (3-4), 165–219 1. doi:10.1016/S0031-0182(01)00208-5

Steiner, M., Yang, B., Hohl, S., Zhang, L., and Chang, S. (2020). Cambrian small skeletal fossil and carbon isotope records of the southern Huangling Anticline, Hubei (China) and implications for chemostratigraphy of the Yangtze Platform. *Palaeogeogr. Palaeocl* 554, 109817. doi:10.1016/j.palaeo.2020.109817

Tarhan, L. G., Droser, M. L., Cole, D. B., and Gehling, J. G. (2018). Ecological expansion and extinction in the late Ediacaran: Weighing the evidence for environmental and biotic drivers. *Integr. Comp. Biol.* 58 (4), 688–702. doi:10.1093/icb/icy020

Taylor, S. R., and McLennan, S. M. (1985). *The continental crust: Its composition and evolution*. Oxford: Blackwell, 312.

Tian, S. P. (1990). Sedimentary facies and sedimentary environment of phosphorite block in Meishucun period of early cambrian in eastern yunnan. *Geol. Chem. Mine* 12, 54–63.

Topper, T., Betts, M. J., Dorjnamjaa, D., Li, G., Li, L., Altanshagai, G., et al. (2022). Locating the BACE of the cambrian: Bayan gol in southwestern Mongolia and global correlation of the ediacaran–cambrian boundary. *Earth-Sci Rev.* 229, 104017. doi:10.1016/j.earscirev.2022.104017

Tostevin, R., Shields, G. A., Tarbuck, G. M., He, T., Clarkson, M. O., and Wood, R. A. (2016). Effective use of cerium anomalies as a redox proxy in carbonate-dominated marine settings. *Chem. Geol.* 438, 146–162. doi:10.1016/j.chemgeo.2016.06.027

Vaziri, S. H., Majidifard, M. R., Darroch, S. A., and Laflamme, M. (2021). Ediacaran diversity and paleoecology from central Iran. *J. Paleontol.* 95 (2), 236–251. doi:10.1017/JPA.2020.88

Veizer, J., Ala, D., Azmy, K., Bruckschen, P., Buhl, D., Bruhn, F., et al. (1999). 87Sr/86Sr, δ^{13}C and δ^{18}O evolution of Phanerozoic seawater. *Chem. Geol.* 161 (1-3), 59–88. doi:10.1016/S0009-2541(99)00081-9

Veizer, J., and Arthur, M. A. (1983). Chemical diagenesis of carbonates: Theory and application of trace element technique. *Stable Isotopes Sediment. Geol.* 1-1, 1–151. doi:10.2110/scn.83.01.0000

Wang, J. Q., and Liu, X. M. (2016). Proficiency testing of the XRF method for measuring 10 major elements in different rock types. *Rock Mine Anal.* 2016, 145–151. doi:10.15898/j.cnki.11-2131/td.2016.02.006

Wang, J., Chen, D., Yan, D., Wei, H., and Xiang, L. (2012). Evolution from an anoxic to oxic deep ocean during the Ediacaran–Cambrian transition and implications for bioradiation. *Chem. Geol.* 306, 129–138. doi:10.1016/j.chemgeo.2012.03.005

Wang, L. Y., Guo, Q. J., Zhao, C. Q., and Yang, X. (2020). Trace and rare Earth elements geochemistry of sedimentary rocks in the Ediacaran-Cambrian transition from Tarim Basin, Northwest China: Constraints for redox environments. *Precambrian Res.* 353, 105942. doi:10.1016/j.precamres.2020.105942

Wang, X., Hu, W., Yao, S., Chen, Q., and Xie, X. (2011). Carbon and strontium isotopes and global correlation of Cambrian Series 2-Series 3 carbonate rocks in the Keping area of the northwestern Tarim Basin, NW China. *Mar. Petro Geol.* 28 (5), 992–1002. doi:10.1016/j.marpetgeo.2011.01.006

Webb, G. E., and Kamber, B. S. (2000). Rare Earth elements in holocene reefal microbialites: A new shallow seawater proxy. *Geochim. Cosmochim. Ac* 64 (9), 1557–1565. doi:10.1016/s0016-7037(99)00400-7

Webb, G. E., Nothdurft, L. D., Kamber, B. S., Kloprogge, J. T., and Zhao, J. X. (2009). Rare Earth element geochemistry of scleractinian coral skeleton during meteoric diagenesis: A sequence through neomorphism of aragonite to calcite. *Sediment* 56 (5), 1433–1463. doi:10.1111/j.1365-3091.2008.01041.x

Wei, G. Y., Planavsky, N. J., Tarhan, L. G., Chen, X., Wei, W., Li, D., et al. (2018). Marine redox fluctuation as a potential trigger for the Cambrian explosion. *Geology* 46 (7), 587–590. doi:10.1130/g40150.1

Wille, M., Nägler, T. F., Lehmann, B., Schröder, S., and Kramers, J. D. (2008). Hydrogen sulphide release to surface waters at the Precambrian/Cambrian boundary. *Nature* 453 (7196), 767–769. doi:10.1038/nature07072

Wood, R., and Erwin, D. H. (2018). Innovation not recovery: Dynamic redox promotes metazoan radiations. *Biol. Rev.* 93 (2), 863–873. doi:10.1111/brv.12375

Wood, R., Liu, A. G., Bowyer, F., Wilby, P. R., Dunn, F. S., Kenchington, C. G., et al. (2019). Integrated records of environmental change and evolution challenge the Cambrian Explosion. *Nat. ecolo Evol.* 3 (4), 528–538. doi:10.1038/s41559-019-0821-6

Wotte, T., Álvaro, J. J., Shields, G. A., Brown, B., Brasier, M. D., and Veizer, J. (2007). C-O-and Sr-isotope stratigraphy across the lower–middle cambrian transition of the cantabrian zone (Spain) and the montagne noire (France), west gondwana. *Palaeogeogr. Palaeocl* 256 (1-2), 47–70. doi:10.1016/j.palaeo.2007.09.002

Yang, B., Steiner, M., Schiffbauer, J. D., Selly, T., Wu, X., Zhang, C., et al. (2020). Ultrastructure of Ediacaran cloudinids suggests diverse taphonomic histories and affinities with non-biomineralized annelids. *Sci. Rep.* 10 (1), 535. doi:10.1038/s41598-019-56317-x

Yang, B., and Steiner, M. (2021). Terreneuvian bio-and chemostratigraphy of the South sichuan region (South China). *J. Geol. Soc.* 178 (5), 167. doi:10.1144/JGS2020-167

Yang, B., Steiner, M., Zhu, M., Li, G., Liu, J., and Liu, P. (2016). Transitional ediacaran–cambrian small skeletal fossil assemblages from South China and Kazakhstan: Implications for chronostratigraphy and metazoan evolution. *Precambrian Res.* 285, 202–215. doi:10.1016/j.precamres.2016.09.016

Zhao, M. Y., and Zheng, Y. F. (2014). Marine carbonate records of terrigenous input into Paleotethyan seawater: Geochemical constraints from Carboniferous limestones. *Geochim. Cosmochim. Ac* 141, 508–531. doi:10.1016/j.gca.2014.07.001

Zhou, C., Xiao, S., Wang, W., Guan, C., Ouyang, Q., and Chen, Z. (2017). The stratigraphic complexity of the middle Ediacaran carbon isotopic record in the Yangtze Gorges area, South China, and its implications for the age and chemostratigraphic significance of the Shuram excursion. *Precambrian Res.* 288, 23–38. doi:10.1016/j.precamres.2016.11.007

Zhou, C., Zhang, J., Li, G., and Yu, Z. (1997). Carbon and oxygen isotopic record of the early Cambrian from the Xiaotan section, Yunnan, South China. *Sci. Geol. Sin.* 204, 201–211.

Zhu, M. (1997). Precambrian–Cambrian trace fossils from eastern yunnan, China: Implications for cambrian explosion. *Bull. Natl. Mus. Nat. Sci.* 10, 275–312.

Zhu, M., Sun, Z., and Yang, A. (2021). Lithostratigraphic subdivision and correlation of the Cambrian in China. *J. Strat.* 2021, 223–249. doi:10.19839/j.cnki.dcxzz.2021.0022

Zhu, M., Yang, A., Yuan, J., Li, G., Zhang, J., Zhao, F., et al. (2019). Cambrian integrative stratigraphy and timescale of China. *Sci. China Earth Sci.* 62 (1), 25–60. doi:10.1007/s11430-017-9291-0

Zhu, M. Y., Babcock, L. E., and Peng, S. C. (2006). Advances in cambrian stratigraphy and paleontology: Integrating correlation techniques, paleobiology, taphonomy and paleoenvironmental reconstruction. *Palaeoworld* 15 (3-4), 217–222. doi:10.1016/j.palwor.2006.10.016

Zhu, M. Y. (2001). Early cambrian stratigraphy of East Yunnan, southwestern China: A synthesis. *Acta Palaeont Sin.* 40, 4–39.

Zhu, M. Y., Zhang, J. M., Li, G. X., and Yang, A. H. (2004). Evolution of C isotopes in the cambrian of China: Implications for cambrian subdivision and trilobite mass extinctions. *Geobios* 37 (2), 287–301. doi:10.1016/j.geobios.2003.06.001

Zhu, M. Y., Zhuravlev, A. Y., Wood, R. A., Zhao, F., and Sukhov, S. S. (2017). A deep root for the Cambrian explosion: Implications of new bio-and chemostratigraphy from the Siberian Platform. *Geology* 45 (5), 459–462. doi:10.1130/G38865.1

Zhu, M., Zhang, J., and Yang, A. (2007). Integrated ediacaran (sinian) chronostratigraphy of SouthSouth China. *Palaeogeogr. Palaeocl* 254 (1-2), 7–61. doi:10.1016/j.palaeo.2007.03.025

Zhu, M., Zhang, J., Yang, A., Li, G., Steiner, M., and Erdtmann, B. D. (2003). Sinian-Cambrian stratigraphic framework for shallow-to deep-water environments of the Yangtze platform: An integrated approach. *Prog. Nat. Sci.* 13 (12), 951–960. doi:10.1080/10020070312331344710

Zhuravlev, A. Y., Liñán, E., Vintaned, J. A. G., Debrenne, F., and Fedorov, A. B. (2012). New finds of skeletal fossils in the terminal Neoproterozoic of the Siberian Platform and Spain. *Acta Palaeont Polo* 57 (1), 205–224. doi:10.4202/app.2010.0074